

Accepted Manuscript

Messinian paleoenvironmental evolution in the lower Guadalquivir Basin (SW Spain) based on benthic foraminifera

José N. Pérez-Asensio, Julio Aguirre, Gerhard Schmiedl, Jorge Civis

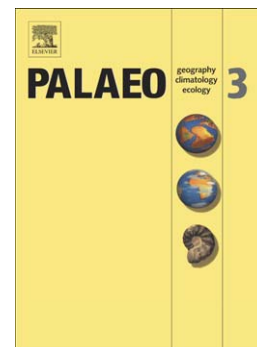
PII: S0031-0182(12)00087-9
DOI: doi: [10.1016/j.palaeo.2012.02.014](https://doi.org/10.1016/j.palaeo.2012.02.014)
Reference: PALAEO 6043

To appear in: *Palaeogeography, Palaeoclimatology, Palaeoecology*

Received date: 22 July 2011
Revised date: 24 January 2012
Accepted date: 11 February 2012

Please cite this article as: Pérez-Asensio, José N., Aguirre, Julio, Schmiedl, Gerhard, Civis, Jorge, Messinian paleoenvironmental evolution in the lower Guadalquivir Basin (SW Spain) based on benthic foraminifera, *Palaeogeography, Palaeoclimatology, Palaeoecology* (2012), doi: [10.1016/j.palaeo.2012.02.014](https://doi.org/10.1016/j.palaeo.2012.02.014)

This is a PDF file of an unedited manuscript that has been accepted for publication. As a service to our customers we are providing this early version of the manuscript. The manuscript will undergo copyediting, typesetting, and review of the resulting proof before it is published in its final form. Please note that during the production process errors may be discovered which could affect the content, and all legal disclaimers that apply to the journal pertain.



Messinian paleoenvironmental evolution in the lower Guadalquivir Basin (SW Spain) based on benthic foraminifera

José N. Pérez-Asensio^{a,*}, Julio Aguirre^a, Gerhard Schmiedl^b and Jorge Civis^c

^a *Department of Stratigraphy and Paleontology, Faculty of Science, Campus de Fuentenueva s.n., University of Granada, 18002 Granada, Spain*

^b *Department of Geosciences, University of Hamburg, 20146 Hamburg, Germany*

^c *Department of Geology, University of Salamanca, 37008 Salamanca, Spain*

* Corresponding author. *E-mail address:* jnoel@ugr.es (José N. Pérez-Asensio).

Telephone: 0034-958-248332. Fax: 0034-958-248528

ABSTRACT

Benthic foraminiferal assemblages of a drill core from the lower Guadalquivir Basin (northern Gulf of Cádiz, SW Spain) have been analysed in order to reconstruct the paleoenvironmental evolution in the vicinity of the Betic seaways during the Messinian. The core consists of marine sediments ranging from the latest Tortonian to the early Pliocene. Changes in the abundance of certain marker species, planktonic/benthic ratio (P/B ratio), paleodepth estimated with a transfer function, content of sand grains and presence of glauconitic layers indicate a complete transgressive-regressive sea-level cycle from the bottom to the top of the section. An abrupt sea-level rise, from inner-middle shelf to middle slope, is recorded at the lowermost part of the core (latest Tortonian-earliest Messinian), followed by a relatively rapid shallowing from middle slope to outer shelf. Magnetobiostratigraphic data show

that this sea-level fall postdates the onset of the Messinian salinity crisis (MSC) in the Mediterranean. Finally, the early Pliocene deposits are interpreted as inner-middle shelf.

Changes in the benthic foraminiferal assemblages through the core are mainly controlled by the trophic conditions, specifically by the quantity and quality of the organic matter reaching the sea floor. The upper slope and part of the outer shelf assemblages are highly diverse and dominated by shallow infaunal species, indicating a generally mesotrophic environment with moderate oxygenation. These environments have likely been affected by repeated upwelling events, documented by increased abundance of *Uvigerina peregrina* s.l., an opportunistic species thriving in environments with enhanced labile organic matter supply. The assemblages of the transitional interval between upper slope to outer-shelf, and of the outer-shelf are generally characterized by a relatively low diversity and epifaunal-shallow infaunal taxa, indicating oligotrophic and well-oxygenated conditions. The inner-middle shelf assemblages are characterized by very low diversity and dominance of intermediate to deep infaunal taxa, suggesting an eutrophic environment with low oxygen content. These assemblages are dominated by *Nonion fabum* and *Bulimina elongata*, two taxa that are able to feed from continental low-quality organic matter, most likely derived from river run-off. The paleoenvironmental evolution on the Atlantic side of Betic and Rifian seaways is similar during the Messinian, with a Messinian continuous sea-level lowering driven by regional tectonic uplift and upwelling-related waters reaching the upper slope. This study will further contribute to understand the role of tectonics on the sea-level changes as well as on the closure of the Atlantic-Mediterranean gateways that led to the MSC, and on the paleoceanography on the Atlantic sides of these corridors.

Keywords: Messinian, benthic foraminifera, salinity crisis, Guadalquivir Basin, SW Spain.

1. Introduction

The Messinian was a time of drastic paleoenvironmental and paleogeographic changes in the Mediterranean (Hsü et al., 1973, 1977). During this time interval, tectonic processes together with glacioeustatic sea-level oscillations led to the isolation of the Mediterranean triggering the formation of thick evaporite deposits during the so-called Messinian salinity crisis (MSC) (Benson, 1986; Benson et al., 1991; Martín and Braga, 1994; Esteban et al., 1996; Riding et al., 1998; Martín et al., 2010). This event took place at around 6 Ma (Gautier et al., 1994; Krijgsman et al., 1999a) as a consequence of the closure of the different gateways connecting the Atlantic and the Mediterranean in the Betic Cordillera in southern Spain (Esteban et al., 1996; Soria et al., 1999; Martín et al., 2001; Betzler et al., 2006; Aguirre et al., 2007; Martín et al., 2009) and the Rifian counterparts in northern Morocco (Benson et al., 1991; Esteban et al., 1996; Krijgsman et al., 1999b; Barbieri and Ori, 2000).

The paleoenvironmental changes that occurred before, during and after the MSC in the Mediterranean and its satellite basins have been intensively studied. Nonetheless, the detailed paleogeographic evolution and the precise timing of the different processes leading to the MSC and the later Mediterranean reflooding are still discussed controversially (Riding et al., 1998; Krijgsman et al., 1999a; Aguirre and Sánchez-Almazo, 2004; Braga et al., 2006; Roveri and Manzi, 2006). Various studies addressed the Messinian paleoenvironmental evolution on the Atlantic side of the Rifian corridors (Hodell et al., 1989; Benson et al., 1991; Gebhardt, 1993; Hodell et al., 1994; Barbieri,

1998; Barbieri and Ori, 2000). The results of these studies show a significant sea-level fall (about 300 m) indicating the onset of the MSC, a reversal water flux through the Rifian corridors and cooling during the Messinian.

The Betic marine passages connected the western Mediterranean with the Atlantic Ocean throughout the Guadalquivir Basin. There are papers dealing with the biochronology of the late Neogene deposits filling the Guadalquivir Basin (Viguier, 1974; Perconig, 1973; Perconig and Granados, 1973; Sierro, 1985; Aguirre et al., 1995; Sierro et al., 1996) and with the tectonostratigraphic framework (Sierro et al., 1996; Riaza and Martínez del Olmo, 1996). However, the available studies on the Messinian paleoenvironmental evolution of the basin are scarce (Berggren and Haq, 1976; Gläser and Betzler, 2002). According to these studies a sea-level drop from middle slope to inner shelf related to the MSC took place during the Messinian.

In this paper, we study the Montemayor-1 core, located in the westernmost part of the northern margin of the Guadalquivir Basin (SW Spain) (Figs. 1 and 2). It covers a complete Messinian sedimentary record (Larrasoña et al., 2008). The location of the core is exceptional to investigate the paleoenvironmental evolution in an area close to the last Betic gateway to be closed, the Guadalhorce corridor (Martín et al., 2001), during the Messinian.

Among the most abundant organisms in the studied sediments are benthic foraminifera. It is largely proved that these organisms are very useful to reconstruct the paleoenvironmental conditions in marine settings, as their distribution depends on several physical, chemical and biological factors (Murray, 1991, 2006). They can be used as proxies of oceanographic parameters such as water depth, substrate, oxygen content and organic matter supply (Jorissen et al., 2007). Thus, the analysis of the variations in the benthic foraminiferal assemblages allows us to infer the key paleoenvironmental factors

controlling their distribution, composition, diversity and microhabitats preferences during the Messinian in an Atlantic-linked basin close to the Guadalhorce corridor. The main objectives of this study are to characterise the benthic foraminiferal assemblages along the core and to assess the changes in the main components of the assemblages in relation with variations in paleoenvironmental parameters, such as sea-level fluctuations, source of organic matter (whether continental or primarily produced in marine contexts), and oxygen content around to the seafloor-substrate interface. This study aims to improve our understanding of the paleoenvironmental and tectonic evolution of the Atlantic-Mediterranean gateways during the MSC, with particular emphasis on the Betic corridor.

2. Study area

The Montemayor-1 core, a continuous core located very close to Moguer (Huelva, SW Spain) (Fig. 2) has been studied. The core was drilled in the northwestern margin of the lower Guadalquivir Basin, an ENE-WSW elongated Atlantic-linked foreland basin of the Betic Cordillera (Sanz de Galdeano and Vera, 1992; Braga et al., 2002). It is limited to the N by the Iberian Massif and to the S by the Subbetic nappes of the Betic Cordillera, and is opened to the Atlantic Ocean to the W (Fig. 1). The Guadalquivir Basin was originated in the earliest Tortonian (late Miocene) as a consequence of the uplifting of the Subbetic Zone of the Betic Cordillera that closed the so-called North Betic Strait (Aguirre et al., 2007; Martín et al., 2009; Braga et al., 2010).

After the closure of the North-Betic Strait, the Guadalquivir Basin was established as a wide, open marine embayment opened to the Atlantic Ocean (Martín et

al., 2009). This basin was filled with marine and continental sediments ranging from the early Tortonian to the late Pliocene (Roldán, 1995; Aguirre et al., 1995; Sierro et al., 1996; González-Delgado et al., 2004). The sedimentary infilling produced a migration of the depocentre approximately along the longitudinal axis of the basin, from the ENE to the WSW. This sedimentary succession has been divided into five depositional sequences (A-E) that have been correlated with third-order cycles of the Haq et al. (1987) global sea-level curve (Sierro et al., 1996).

In Huelva and neighbouring areas, the Neogene deposits have been divided into four lithostratigraphic units formally described as formations. The lowermost unit is the Niebla Formation (Civis et al., 1987; Baceta and Pendón, 1999). It consists of late Tortonian carbonate-siliciclastic mixed deposits that unconformably onlap the Paleozoic-Mesozoic basement of the Iberian Massif (Baceta and Pendón, 1999). The second unit, latest Tortonian-Messinian according to planktonic foraminifera and calcareous nannoplankton (Sierro, 1985, 1987; Flores, 1987; Sierro et al., 1993), is the Arcillas de Gibraleón Formation (Civis et al., 1987). This unit, which begins with 2-4 m of glauconitic silts (Baceta and Pendón, 1999), consists mostly of greenish-bluish clays. The third unit is the Arenas de Huelva Formation (Civis et al., 1987) that includes early Pliocene silts and highly fossiliferous sands. A glauconite-rich layer is found at the lowermost part of the formation. Finally, this unit is unconformably overlain by sand of the uppermost unit, the Arenas de Bonares Formation, which is attributed to the late Pliocene with no biostratigraphic precision (Mayoral and Pendón, 1987).

3. Stratigraphy of the Montemayor-1 core

The Montemayor-1 core ranges from the latest Tortonian to the Zanclean (Larrasoña et al., 2008) (Fig. 3). The age of the core is well constrained based on magnetobiostratigraphic methods. The magnetostratigraphic dating was performed with the revised astronomically-tuned geomagnetic polarity timescale of Lourens et al. (2004) (ATNTS2004). The paleomagnetic record of the core comprises from the upper part of the C3Br.2r (ca. 7.4 Ma) to the C3n/C2Ar boundary (ca. 4.3-4.2 Ma) (Larrasoña et al., 2008) (Fig. 3). The biostratigraphic framework is based on planktonic foraminiferal (PF) events 3, 4 and 6 of Sierro et al. (1993), and the first occurrence of *Globorotalia puncticulata*. According to these authors, the PF event 3, which is correlated with the Tortonian/Messinian boundary, is the replacement of the *Globorotalia menardii* group II by the *Globorotalia miotumida* group; the PF event 4 is the first abundant occurrence of dextral specimens in the *Neogloboquadrina acostaensis* group; and the PF event 6 is first abundant occurrence of *Globorotalia margaritae* s.s.

The Montemayor-1 core is 260 m long including the uppermost part of the basement and the marine sediments of the four aforementioned formations (Fig. 3). The core begins with 1.5 m of reddish clays from the Paleozoic-Mesozoic substrate. A well-cemented sandy calcarenite layer 0.5 m thick, corresponding to the Niebla Formation, unconformably overlays the basement. Silt and clay belonging to the Arcillas de Gibraleón Formation, 198 m in thickness, overlay the sandy calcarenites. A glauconitic layer, 3 m in thickness, is present at the base of the formation. The sharp boundary between the Niebla and Arcillas de Gibraleón formations, located at 258 m, could be correlated with the unconformity observed in coeval deposits cropping out onland (Baceta and Pendón, 1999). Sands and silts from the Arenas de Huelva Formation, 42 m thick, overlay the underlying formation. A 3 m-thick glauconitic layer is found at the base of the unit. According to the paleomagnetic data, a discontinuity, located at 60 m,

separates these deposits from the Arcillas de Gibraleón (Larrasoña et al., 2008). The Montemayor-1 core ends with 14.5 m of brownish sands with marine fossils, the Arenas de Bonares Formation which presents a discontinuity at the bottom (18 m), and 3.5 m of recent soil.

Sedimentation rate was estimated in cm/kyr using thickness of paleomagnetic chrons and the calibrated time scale in Fig. 3. Sedimentation rate was calculated in 3 intervals: 1) from the bottom of the chron C3Br.1n to the top of the chron C3Ar; 2) from the bottom of the chron C3An to the top of the chron C3An; and 3) from the bottom of the chron C3r to the top of the chron C3r (Fig. 3). Concerning the three discontinuities of the core, the lower and upper discontinuities, located at 258 and 18 m respectively, prevent us from estimating the sedimentation rate for the lowermost and uppermost parts of the core (Fig. 3). The sedimentation rate for the chron C3r is also uncertain because of the discontinuity located at 60 m (Fig. 3).

4. Methods

In this paper, an interval of 220 m, from 256.5 m to 36.5 m in the core, has been studied. This interval encompasses the Arcillas de Gibraleón, and the lower part of the Arenas de Huelva. According to the magnetobiostratigraphy, the sedimentary record of the studied interval is continuous except for a discontinuity close to the Miocene-Pliocene boundary, located at 60 m (Fig. 3). A total of 89 samples each 2.5 m have been analysed. All samples were washed over a 63 μm sieve and oven dried at 40 °C.

For faunal analysis, samples were divided into equal aliquots with a microsampler to obtain sub-samples containing at least 300 benthic foraminifera. These sub-samples were dry-sieved over a 125 μm sieve, and benthic foraminifera were

identified and counted. Census data were transformed into relative abundances. Several metrics were calculated: 1) number of taxa (species richness), 2) the Shannon index (H):

$$H = -\sum p_i \ln p_i$$

where p_i is the proportion of the i^{th} species and \ln is the natural logarithm; 3) evenness (E) *sensu* Hayek and Buzas (1997):

$$E = e^H/S$$

where e is the base of the natural logarithms, H is the Shannon index, and S is the number of species; and 4) the dominance (D), defined as the percentage of the most abundant species (Levin and Cage, 1998), has also been quantified.

The sand content was determined as percentage of the $> 63 \mu\text{m}$ fraction. The total number of benthic foraminifera per gram of dry sediment (N/g) was also calculated.

Changes in paleowater depth have been inferred applying various proxies, including the planktonic/benthic ratio (P/B ratio hereafter), specific marker taxa with a narrow and well-defined depth distribution range (depth markers), and a quantitative transfer function based on benthic foraminiferal depth ranges. The P/B ratio, scored as $[P/(P+B)]$, was used as an approximation to infer sea-level changes. The use of P/B ratio to represent sea-level changes exhibits many drawbacks. For instance, dissolution affects preferentially to planktic foraminifera (Kucera, 2007), and the planktic foraminifera abundance decreases in brackish waters (Arnold and Parker, 1999; Retailleau et al., 2009). Furthermore, benthic foraminiferal abundance interferes with oxygen and food levels at the sea floor affecting the P/B ratio (van Hinsbergen et al., 2005; Milker, 2010). In spite of these limitations, the P/B ratio can be used to infer general sea-level trends. Depth markers can be used for a qualitative estimation of water depth, notwithstanding their occurrence can be related to environmental conditions

instead of water depth, such as oxygen and organic matter supply (van Hinsbergen et al., 2005). In order to define depth markers, we discarded species with a wide bathymetric range such as bolivinids, buliminids and uvigerinids. Depth markers used in this study are: 1) *Ammonia beccarii* and *Ammonia* sp (inner-middle shelf); 2) *Cibicidoides floridanus* (outer shelf); 3) *Planulina ariminensis* (predominantly upper slope); 4) *Anomalinoidea flinti* (middle and lower slope); 5) *Oridorsalis umbonatus* and *Siphonina reticulata* (predominantly middle and lower slope). Finally, the transfer function developed by Hohenegger (2005) based on depth ranges of benthic foraminiferal taxa, later modified by Báldi and Hohenegger (2008) and Hohenegger et al. (2008) to include the species relative abundances, was applied to quantitatively estimate sea-level fluctuations:

$$\text{paleodepth (m)} = \frac{\sum(n_j l_j d_j^{-1})}{\sum(n_j d_j^{-1})}$$

where n_j is the relative abundance of the j^{th} species, l_j is the geometric average of the distribution borders, and d_j is the dispersion. For the transfer function, very rare species were not used, only species with $\geq 1\%$ of the total assemblage at least in 3 samples were considered (Table 1). Following the recommendations made by Hohenegger (2005), we use global data of water-depth distribution of benthic foraminifer species, thus, avoiding local or geographical biases in their bathymetric ranges. Thus, we consider the largest depth range possible for each species (Table 1). The accuracy of the water depth estimates was expressed with the 95% confidence intervals (Table 2).

The major limitation for the quantitative transfer function is that for living taxa is based on modern depth ranges and for extinct taxa is calculated comparing with depth ranges of morphologically most similar living counterparts (Hohenegger et al., 2008). Nevertheless, almost all of the taxa we found are not extinct and we assume that their depth ranges have not substantially changed through time. Another limitation is that

transported shallow-water taxa produce an underestimation of water depth. This problem was solved removing allochthonous taxa before applying the equation. Allochthonous species are those with a depth range that is different and does not overlap the depth range of the autochthonous species found in each sample. Taking these limitations into consideration, the application of the transfer function to several case studies has proved to be a powerful tool to quantitatively estimate paleodepth (Hohenegger, 2005; Spezzaferri and Tamburini, 2007; Hohenegger et al., 2008; Báldi and Hohenegger, 2008).

Q and R-mode principal component analyses (PCA) were performed to determine the benthic foraminiferal assemblages using the software package SYSTAT 12. The Q-mode PCA groups the dominant species into assemblages. In the R-mode PCA, species with similar distribution patterns independent from their relative abundance are grouped together. To remove the effect of very rare species, only those representing $\geq 1\%$ of the total assemblage at least in 3 samples were considered. Pearson correlation coefficients were calculated to quantify the relationships between all the metrics used in this study. Correlations with a p -value < 0.01 were considered significant.

Benthic foraminifera were classified according to their microhabitat preferences (Table 3). Five different microhabitats have been recognized, following Lutze and Thiel (1989) and Schmiedl et al. (2000): a) epifaunal, elevated epibenthic species, b) epifaunal-shallow infaunal (0-0.7 cm below the water-sediment interface; BWSI), c) shallow infaunal (0.7-1.5 cm BWSI), d) intermediate infaunal (1.5-3 cm BWSI), and e) deep infaunal (>3 cm BWSI).

5. Results

Results of the measured parameters allow the division of the studied section into three intervals: a) The lower interval is from 256.5 m, the base of the core, to 180 m. This ranges the latest Tortonian and lower part of the Messinian. b) The middle interval is from 180 to 60 m. This includes the upper part of the Messinian up to the unconformity detected close to the Miocene-Pliocene boundary. c) The upper interval is from 60 m to the end of the section, 36.5 m, that corresponds with the lower part of the Pliocene deposits. For practical reasons, in the description and discussion following below, we will refer to these three parts or intervals.

5.1. Numerical faunal parameters, sand content, and sedimentation rate

The P/B ratio shows a very sharp increase in the lowermost part, with maximum values around 0.6, followed by a gradual decrease to values between approximately 0.1 and 0.3 in the middle and uppermost part of the section. The lowest P/B ratios (< 0.1) appear in the upper part of the section (Fig. 4). The sand content is lower than 5% throughout most of the core, except in the two first samples, at 256.5 and 254 m (nearly 50%), and in the upper part of the section (fluctuating values with up to 38%). The total number of benthic foraminifera per gram of dry sediment (N/g) shows high values in the lower part (> 50 N/g as an average) of the core. The middle part of the section starts with values below 50 N/g and ends with values above 50 N/g. Fluctuating values (mostly higher than 50 N/g) are recorded in the upper part of the section.

In the lowermost part of the core (256.5-240 m), the estimated sedimentation rate shows the lowest values throughout the section, with 2.7 cm/kyr (Fig. 3). The estimated sedimentation rate exhibits an abrupt increase at 217.5 m, corresponding to the base of chron C3r, changing from 3.2 cm/kyr to 20 cm/kyr (Fig. 3). This significant

change in sedimentation rate is also detected by a sharp decrease in natural remanent magnetization intensities (Larrasoña et al., 2008).

5.2. *Species richness, diversity and dominance*

In the lower part of the section, the number of taxa ranges between 40 and 50, followed by a decrease with values ranging between 30 and 40. In the middle part, the values fluctuate around 40. In the upper part, the number of taxa first decreases sharply, reaching the lowest values (< 30) between approximately 60 and 45 m, followed by increased values > 30 (Fig. 5).

The Shannon index (H) and the evenness (E) have very similar trends as they show a positive high Pearson correlation coefficient (Table 4), but fluctuations in the evenness are more expressed (Fig. 5). Both H and E decrease progressively through the lower part of the core. In the middle part, both metrics alternate between relatively higher, then lower and finally higher values. In the upper part, H and E sharply decrease reaching the lowest values (H=0.93, E=0.18). Above this low diversified interval, both parameters abruptly increase. The dominance shows an opposite trend as those shown by H and E. This is consistent with the negative high Pearson correlation coefficients (Table 4).

5.3. *Benthic foraminiferal assemblages*

The Q-mode PCA yields 3 assemblages that explain 81.8 % of the total variance (Table 5). The *Cibicidoides pachyderma* assemblage (PC1), with *Cibicidoides* sp., *Cibicidoides floridanus* and *Brizalina spathulata* as accompanying species (Figs. 6A-

6D, Table 5), shows a fluctuating pattern in the lower part and becomes dominant in the middle part of the core (Fig. 7). The *Nonion fabum* assemblage (PC2) includes *Ammonia beccarii*, *Spiroplectinella* sp., *Ammonia* sp., *Bulimina elongata* and *Brizalina spathulata* as associated taxa (Figs. 6D-6H, Table 5). This assemblage is important in the lowermost sample and in the upper part of the section (Fig. 7). The *Uvigerina peregrina* s.l. assemblage (PC3) dominates the lower part and shows significant values in the middle part, between 160 and 140 m (Fig. 7). *Bulimina subulata*, *Cibicidoides pachyderma*, *Planulina ariminensis* and *Cibicidoides* sp. are the associated taxa (Figs. 6A-6B, 6I-6K, Table 5).

The relative abundances of dominant and associated taxa from Q-mode assemblages are shown in Fig. 8. Three distinctive patterns of relative abundance can be distinguished. The first group of species dominates in the lower part of the core, comprising *Uvigerina peregrina* s.l. (*Uvigerina peregrina*+*Uvigerina pigma*), *Bulimina subulata* and *Planulina ariminensis*. The latter species is exclusively limited to this part of the core (Fig. 8). The second group of species is important throughout the section, except in the upper part, comprising *C. pachyderma*, *Cibicidoides* sp., and in lesser abundance *C. floridanus*. The third group of species dominates in the upper part of the section, comprising *A. beccarii*, *Ammonia* sp., *Spiroplectinella* sp., *B. elongata*, *N. fabum* and *B. spathulata*. Among them, *N. fabum* reaches the highest values when the others show low percentages (Fig. 8). These species show also a peak of abundance in the first sample of the core.

The R-mode PCA explains 31.2 % of the total variance and differentiates 3 assemblages (Fig. 9, Table 6). The *Anomalinoidea flinti* assemblage (PC2) is only important in the lower, part between 254 and 211.5 m (Fig. 9). Some of the associated taxa of this assemblage are *Siphonina reticulata*, *Oridorsalis umbonatus*, *Uvigerina*

striatissima and *Planulina ariminensis* (Figs. 6K, 6O-6R, Table 6). In the middle part, the *Cibicidoides pachyderma* assemblage (PC3) becomes significant (Fig. 9).

Cibicidoides floridanus and *Hanzawaia boueana* are other important taxa of this assemblage (Figs. 6A-6C, 6S, Table 6). In the upper part, from 44 m to the top, the *Spiroplectinella* sp. assemblage dominates (PC1) (Fig. 9). This assemblage includes *Valvulineria complanata*, *Textularia* sp., *Melonis barleeaanum*, *Textularia agglutinans*, *Cassidulina laevigata* and *Ammonia beccarii* as secondary species (Figs. 6G, 6L-6N, Table 6).

5.4. Estimated paleodepth

A water depth of 31.88 m is estimated for the lowermost sample (Fig. 10, Table 2). Then, paleodepth sharply increases reaching 449.67 m, and decreases to 282.82 m at the end of the lower part. An important sea-level lowering is detected at 211.5 m, in the middle part of the lower interval, followed by a rapid increment up to 375.50 m. Paleodepth suddenly diminishes at the beginning of the middle part, then slightly decreases and finally abruptly drops to 37.94 m. In the upper part, paleodepth remains stable with values between 40 and 50 m, except for the last two samples that has values around 12 m (Table 2).

5.5. Distribution of benthic foraminiferal microhabitats

The lowermost sample has a high percentage of intermediate infaunal species (Fig. 11). In the lower part of the core, between 254 to 194 m, shallow infaunal taxa show high percentages and epifauna only amounts to 10 % on average. Between 194

and 180 m, the epifauna and epifauna-shallow infauna increase, and the shallow infauna decreases. In the middle part of the core, between 165 and 130 m, the shallow infauna has relatively high values. Up in the section, epifaunal-shallow infaunal species become significant but then gradually diminish, being replaced by shallow infauna towards the top of the middle part (around 60 m). In the upper part, between 64.5 and 46.5 m, intermediate infaunal species are significantly abundant, reaching up to 80 %. In this interval, deep infauna also reaches the highest values. From 56.5 to the top of the core, the fauna is dominated by shallow infaunal and epifaunal-shallow infaunal taxa (Fig. 11).

6. Discussion

6.1. Relative sea-level fluctuations

According to the paleobathymetric indicators used in this study, a very abrupt sea-level rise is inferred at the lowermost part of the core. The Q-mode PCA *Nonion fabum* assemblage, which includes species inhabiting inner-middle shelf such as *Ammonia beccarii* and *Ammonia* sp. (Murray, 1991, 2006), occurs in the lowermost sample of the section (Fig. 7, Table 5). A peak in sand content in this sample (Fig. 4) is consistent with a shallow inner-middle shelf paleoenvironment. Further, this is supported by a paleodepth of 31.88 m estimated with the transfer function (Fig. 10, Table 2). Coincidentally, a very low value of the P/B ratio is also shown (Fig. 4).

The next three samples show a significant increase in the *Cibicidoides pachyderma* assemblage that includes *Cibicidoides floridanus*, a species living on the outer shelf (van Morkhoven et al., 1986; Barbieri and Ori, 2000), as associated species

(Fig. 7, Table 5). Coinciding with the increased importance of this assemblage, the P/B ratio and paleodepth rise concomitantly (Figs. 4 and 10), responding to the rapid sea-level rise. Sand-sized particles virtually disappear, which is consistent with the inferred deepening (Fig. 4).

Enhanced glauconite concentration is recorded in the second sample of the section. Glauconite is commonly formed along the shelf to continental slope during transgressions and under very low sedimentation rates (Odin and Matter, 1981; Galán et al., 1989; Harris and Whiting, 2000). The rapid transgression produced a sharp onshore shift of the depositional systems, trapping the coarse-grained sediment in shallower areas of the platform. Sedimentation rate dropped and sand grains virtually disappeared in this interval (Figs. 3, 4), thus promoting the deposition of glauconite. As a recent analogue, glauconite is formed on the present-day outer shelf off Guadiana River (SW Spain), close to the study area (Gonzalez et al., 2004).

Magnetobiostratigraphic data indicate that the rapid sea-level rise occurred during the latest Tortonian-earliest Messinian. The same sea-level rise has been also inferred from the investigation of onland sections along the northern margin of the lower Guadalquivir Basin (Baceta and Pendón, 1999; González-Regalado et al., 2005).

The maximum flooding is reached between 254 and 236.50 m core depth as indicated by the dominance of the *Anomalinoides flinti* R-mode assemblage (Fig. 9), and the highest paleodepth values (Fig. 10, Table 2). *Anomalinoides flinti* is common in middle and lower slope settings (Berggren and Haq, 1976). Some additional taxa of this assemblage (Table 6), such as *Siphonina reticulata* and *Oridorsalis umbonatus*, also inhabit the middle and lower slope (Berggren and Haq, 1976; Berggren et al., 1976; Hayward et al., 2003). This assemblage shows a positive Pearson correlation coefficient with P/B ratio (Table 4) and dominates at highest P/B ratios (Fig. 4). Consequently,

maximum flooding detected in this part of the core reached at least the middle talus slope.

Following the maximum flooding, the P/B ratio and paleodepth decrease progressively up to the end of the lower core interval, suggesting a sea-level lowering (Figs. 4 and 10). This interpretation is supported by a decrease of the *A. flinti* assemblage scores (Fig. 9). The dominance of the *U. peregrina* s.l. assemblage in this part of the section (Fig. 7) suggests an upper slope depositional environment. Similarly, *Planulina ariminensis* (Table 5), an associated species of the *U. peregrina* s.l. assemblage, predominantly inhabits the upper slope, with maximum abundances commonly between 300-500 m (Berggren and Haq, 1976; Schönfeld, 1997). The same bathymetric preference of *P. ariminensis* was also inferred for occurrences in Miocene-early Pliocene deposits off Morocco (Gebhardt, 1993). This species also inhabits the upper slope in the continental margins off NW Africa, off southern Portugal, and in the Gulf of Cádiz (Lutze, 1980; Schönfeld, 1997, 2002). Quantitative transfer function also suggests an upper slope water depth between 400 and 250 m (Fig. 10, Table 2). Coincidentally, *U. peregrina* is below 300 m depth in the Gulf of Mexico (Parker, 1954; Schönfeld, 2006).

In the last ten meters of the lower interval, 190-180 m, the P/B ratio, estimated paleodepth, and the *U. peregrina* s.l. assemblage decrease rapidly (Figs. 4, 7 and 10, Table 2). All these changes are interpreted as a sea-level fall. Concurrently, the *Cibicidoides pachyderma* assemblage dominates, as documented by the Q-mode assemblage (Fig. 7). Above this benthic foraminifera faunal turnover, at 179 m, *P. ariminensis* disappears (Fig. 8), thus indicating the transition to the outer shelf, and corroborating the sea-level decrease. At the north of Cape Blanc in the continental

margin of NW Africa the shallowest occurrence of *P. ariminensis* also indicates the transition to the outer shelf (Lutze and Coulbourn, 1984).

This sea-level drop occurred in chron C3r (Fig. 10, Table 2). Therefore the age uncertainty for this event is from 6.033 to 5.235 Ma. However, it can be correlated with the global sea-level fall that took place during the mid Messinian (Haq et al., 1987; Hardenbol et al., 1998) (Fig. 10). At the northwestern margin of Morocco, Barbieri and Ori (2000) also detected a sea-level fall during the middle part of the Messinian that can be correlated with the sea-level drop observed in the Montemayor-1 core (Fig. 10). These authors associated the mid-Messinian shallowing with the onset of the MSC on the Atlantic side of the Rifian corridors and correlated it with the glacial stages TG22 and TG20 of Shackleton et al. (1995), two of the most pronounced glacial events occurring during the Messinian. Nonetheless, these glacial stages have been dated at 5.79 and 5.75 Ma, respectively (Krijgsman et al., 2004), well after the onset of the MSC that took place at 5.96 ± 0.02 Ma according to Krijgsman et al. (1999a). Hence, the major sea-level fall observed both in the Montemayor-1 core and in the Rifian corridors would most likely postdate the start of the MSC. The detailed record along the core of the estimated paleodepth trend based on the transfer function allows us to identify a major sea-level fall at 211.5 m, before the aforementioned major sea-level drop (Fig. 10, Table 2). This sea-level fall could be related to the onset of the MSC.

In spite of the constant dominance of the outer shelf *C. pachyderma* assemblage throughout the middle core interval, the continuous upward decrease in P/B ratios and paleodepth (Figs. 4 and 10) suggests a slight and progressive lowering in sea level. The middle core interval ends with a sharp sea-level fall reaching the middle shelf. This shallowing is also recorded in the Rifian corridors (Fig. 10).

The continuous Messinian record is interrupted by a discontinuity around the Miocene-Pliocene boundary (Fig. 3). After this unconformity, an inner-middle shelf setting established during the deposition of the upper part of the section. This setting is indicated by the dominance of the *Nonion fabum* assemblage (Fig 7), and paleodepth values between 40 and 50 m (Fig. 10, Table 2).

The glauconitic layer at the base of the upper part of the core caps the unconformity (Figs. 3). This bed is also present in onland sections and has been interpreted as the transgressive deposits formed during the early Pliocene (Sierro and Flores, 1992; Sierro et al., 1996). Nonetheless, this deepening did not exceed the early Messinian inundation since only shelf deposits were formed during the early Pliocene at the studied site.

The global sea-level curve of Hardenbol et al. (1998) shows three transgressive-regressive 3rd-order cycles during the late Tortonian-early Pliocene (Fig. 10). This global trend is not recorded in the Montemayor-1 core. As previously discussed, sea-level at the Montemayor-1 core site shows a very rapid rise close to the Tortonian-Messinian boundary, when the global sea-level curve shows a progressive shallowing (Fig. 10). After the sudden deepening in the Montemayor-1 core, sea-level followed a continuous fall until the end of the Messinian (Fig. 10). The Handerbol et al. (1998) eustatic curve shows, however, a fluctuating sea level. Gebhardt (1993) and Barbieri and Ori (2000) noticed a similar Messinan sea-level trend in the Atlantic side of the Rifian corridors as that observed in Montemayor-1 core, thus differing from the global one. According to these authors, a regional tectonic uplifting might account for the continuous sea-level drop through the Messinian in a context of global fluctuating sea level. Tectonic uplifting also led to the closure of the Guadalhorce corridor during the Messinian, most likely just before the main gypsum deposition in the Mediterranean

(Martín et al., 2001). The N-S compressional regime established during the Messinian in the Betic-Rifean domain (Sanz de Galdeano, 1990; Maldonado et al., 1999) supports this interpretation. Thus, our data sustain that the tectonic uplift could played an important role in the relative sea-level changes observed in the Atlantic side of the Atlantic-Mediterranean gateways in both the Rifian corridors and the Betic ones. This might explain the age disagreement between the major sea-level fall observed during the mid Messinian and that leading to the onset of the MSC.

6.2. Paleoenvironmental key factors: continental versus marine organic matter supply and seafloor oxygen content

It is well known that organic matter supply and dissolved oxygen content in the sea bottom and pore waters are among the key environmental factors affecting benthic foraminifera distribution (e.g., Jorissen et al., 1995; Fariduddin and Loubere, 1997; De Rijk et al., 2000; Jorissen et al., 2007). The impact of these factors on benthic foraminifera cannot be analysed separately. The oxygen content of the sea floor and in the pore waters is controlled by the quantity of organic matter. In environments with high organic input, the remineralisation of organic matter decreases the oxygen concentration on the sea floor as well as the depth of oxygen penetration below the water-sediment interface (Jorissen et al., 1995; Mojtahid et al., 2009, 2010a). Consequently, eutrophic environments are commonly characterised by a low oxygen concentration and shallow oxygen penetration, while oligotrophic environments exhibit a high oxygen concentration and deep oxygen penetration. Furthermore, changes in the trophic conditions can produce variations in the diversity and microhabitat preferences. Oligotrophic environments are dominated by epifaunal taxa and have rather low

diversity; mesotrophic environments show the highest diversity and all microhabitats are represented; and finally, eutrophic environments are characterised by low diversity and dominance of (deep) infaunal taxa (Jorissen et al., 1995).

Based on this concept, it appears likely that the benthic foraminiferal fauna at the study site was also influenced by changes in trophic conditions, particularly in quantity and quality of the available food source. In general, continental organic matter is more refractory than organic matter primarily produced in marine settings since terrestrial-derived organic matter is degraded before reaching the marine environment (Zonneveld et al., 2010). High input of this terrestrial organic matter can provoke eutrophication and led to oxygen depletion at the bottom and pore waters (Van der Zwaan and Jorissen, 1991; Jorissen et al., 1992; Donnici and Serandrei Barbero, 2002)

The inner-middle shelf *Nonion fabum* assemblage at the base of the section (Fig 7) indicates the most eutrophic conditions, suggesting organic matter run-off from the continent. This assemblage is characterised by low diversity and dominance of intermediate infaunal taxa (Figs. 5 and 11). *Nonion fabum* is usually associated with eutrophic environments with high organic matter of low quality and significant oxygen depletion (Fontanier et al., 2002; Duchemin et al., 2008; Mojtahid et al., 2010a, 2010b). In the prodelta of the Rhône River, high proportions of *N. fabum* occur under the influence of the river plume reflecting low-quality continental organic matter supply from river discharge and low oxygen penetration (Mojtahid et al., 2010b; Goineau et al., 2011). Similarly, *Bulimina elongata*, an associated species of the *N. fabum* assemblage, can also feed from low quality organic matter and tolerates low oxygen concentrations (Diz and Francés, 2008; Mojtahid et al., 2009). Coincidentally, *B. elongata* also occurs in the Rhône prodelta close to the river mouth (Mojtahid et al., 2009).

Above the *N. fabum* assemblage, the *Uvigerina peregrina* s.l. and the *Cibicidoides pachyderma* assemblages alternate (Fig. 7). *Uvigerina peregrina* s.l. is an opportunistic taxon commonly present in fine grained sediments deposited in environments with significant fluxes of labile organic matter and moderate oxygen depletion (Schmiedl et al., 1997, 2000; 2010; Fontanier et al., 2002; Koho et al., 2008). The presence of *Uvigerina peregrina* s.l. indicates a productivity between 4.0 to 17.0 g C m⁻² yr⁻¹ in NW-Africa and Gulf of Guinea and from 4.0 to 5.1 g C m⁻² yr⁻¹ in the northeastern Atlantic (Schönfeld and Altenbach, 2005). Furthermore, this species is common in upper slope and outer shelf environments under the influence of seasonal upwelling events, for example off Southwest Africa (Schmiedl et al., 1997), off the Ría de Vigo, NW Spain (Martins et al., 2006), off Congo (Mojtahid et al., 2006), and off the Guadiana platform, SW Spain (Mendes et al., 2004), close to the study area.

Accordingly, the presence of upwelling above the upper slope may account for the dominance of *U. peregrina* s.l. assemblage in the lower part of the section. This assemblage indicates mesotrophic conditions, characterised by a relatively high benthic foraminiferal diversity and low dominance (Fig. 5), as well as the highest percentages of shallow infaunal taxa (Fig. 11). The high abundance of shallow infaunal taxa in mesotrophic settings is attributed to a diversification of infaunal niches (Milker et al., 2009). The present-day current system in the northern Gulf of Cádiz can be used as a possible analogue for the paleoceanographic setting in the study area during the Messinian. In the present Gulf of Cádiz, major upwelling is located near Cape St. Vicent (S Portugal), and during westerly conditions, upwelled waters extend eastwards along the shelf margin reaching our study area (Vargas et al., 2003; Criado-Aldeanueva et al., 2006).

On the other hand, the *C. pachyderma* assemblage shows a high abundance of epifaunal-shallow infaunal taxa and relatively low diversity indicating more oligotrophic conditions (Figs. 5 and 11). *Cibicidoides pachyderma* is a suspension feeder that inhabits oligo- to mesotrophic environments with high oxygenation contents (Gebhardt, 1999; Schmiedl et al., 2000, 2003). This species feeds from episodic inputs of labile organic matter (Fontanier et al., 2002; Melki et al., 2009). The presence of *Cibicidoides* sp. is also consistent with a well-oxygenated and relatively oligotrophic setting (Kaiho, 1994, 1999; Takata, et al., 2010). To summarize, the alternation of *U. peregrina* s.l. and *C. pachyderma* assemblages in the lower part of the section suggests episodic influence of upwelling currents and related food pulses at the core site.

At the end of deposition of the lower core interval (194-180 m), the influence of upwelling currents diminished, indicated by the disappearance of the *U. peregrina* s.l. assemblage and the consistent establishment of the *C. pachyderma* assemblage. This faunal turnover coincides with a maximum proportion of epifaunal taxa in the interval between 194 and 180 m, attributable to the high abundance of the epifaunal species *Planulina ariminensis* (Figs. 7, 8 and 11). This transition interval likely represents particularly oligotrophic conditions.

The outer shelf *C. pachyderma* assemblage dominates throughout the middle part of the section (180-60 m), although some short-term occurrences of the *U. peregrina* s.l. assemblage are observed between 160 and 140 m.

Similarly, the sporadic influence of upwelling currents likely also fostered high diversity and increase of shallow infaunal species, such as *B. spathulata*, at the end of deposition of the middle core interval (120-60 m) (Figs. 5, 8 and 11). *Brizalina spathulata* can tolerate low oxygen concentrations (Barmawidjaja et al., 1992;

Stefanelli, 2004) and shows an opportunistic life style, rapidly responding to pulses of fresh organic matter in high oxygen environments (Fontanier et al., 2003; Diz et al., 2006; Diz and Francés, 2008). In the Ría de Vigo (NW Spain), this species reproduces immediately after phytoplankton blooms related to upwelling conditions (Diz et al., 2006; Diz and Francés, 2008). It is also related to upwelling events off Guadiana River in SW Iberia (Mendes et al., 2004). However, the increased abundance of *B. spathulata* could also be related to nutrient influx derived from the continent as has been observed by other authors (i.e. Duchemin et al., 2008; Schmiedl et al., 2010).

During deposition of the upper part of the section (60-36.5 m), the inner-middle shelf was inhabited by the *N. fabum* assemblage indicating eutrophic conditions. Here, species dominance and percentages of deep and intermediate infauna reach maximum values (Figs. 5 and 11). *Nonion fabum* is found in the finer-grained interval, between 56.5 and 39 m (Figs. 4 and 8), consistent with its preference to muddy sediments (Haunold et al., 1997; Rezqi et al., 2000; Duchemin et al., 2008). In the present-day northern and northeastern Gulf of Cádiz, extensive mud deposits accumulate on the middle shelf, related to the Guadiana run-off (Gonzalez et al., 2004) and to the Guadalquivir prodelta (Gutiérrez-Mas et al., 1996; Nelson et al., 1999). Recent *N. fabum* populations proliferate in the prodelta muddy sediments of the Guadalquivir River (Villanueva-Guimerans and Canudo, 2008). In late Pliocene deposits from the Almería-Níjar basin (SE Spain), *N. fabum* is a major component in silts and fine-grained sands of middle fan-delta deposits and in varve-like laminated deposits that indicate low-oxygen conditions and high organic input derived from terrestrial run-off (Pérez-Asensio and Aguirre, 2010). Hence, the dominance of this species in the upper part of the studied section points to periods of high river run-off supplying fine-grained sediment and low quality continental organic matter.

The interpretation of river-derived continental matter input is corroborated by appearance of *B. elongata* that has been observed in comparable environments of the Mediterranean Sea (Jorissen, 1988; Mojtahid et al., 2009). Enhanced river run-off influence is also suggested by the low P/B ratio values in the muddy interval (Fig. 4), because planktic foraminifera do not tolerate brackish waters (Arnold and Parker, 1999; Retailleau, et al., 2009).

The upper limit of the muddy interval is dominated by the R-mode *Spiroplectinella* assemblage, coinciding with a sandy substrate and high diversity (Figs. 4, 5 and 9). *Valvulineria complanata* and *Textularia* sp. (Table 6) are also abundant in this assemblage. In the prodelta of the Rhône River, *V. complanata* and some arenaceous taxa, such as *Textularia agglutinans* and *Textularia porrecta*, occur close to the end of the freshwater layer entering the marine waters. Food supply in this environment is mainly of marine origin although there is still influence of organic matter provided from the continent (Mojtahid et al., 2009, Goineau et al., 2011). Thus, the *Spiroplectinella* sp. assemblage is indicative of shallow freshwater-marine transitional conditions with a greater influence of marine organic matter in a sandy inner shelf environment.

Benthic foraminiferal assemblages of the Montemayor-1 core show a mesotrophic upper slope setting influenced by seasonal upwelling, an oligotrophic outer shelf less affected by upwelling, and inner-middle shelf settings with high continental run-off influence. Upwelling conditions also prevailed on the upper slope of the Atlantic side of the Rifian corridors during the Messinian (Gebhardt, 1993). The coastal upwellings have persisted off NW Africa up to the present day (Sarnthein et al., 1982). In our study case, however, it seems that the position of the area of major influence of upwelling nuclei has changed westwards from the Messinian to the recent. This

paleoceanographic reconfiguration in the northern Gulf of Cádiz can be due to the observed Messinian progressive shallowing. This is consistent with the change in organic matter supply from marine labile to continental refractory inferred along the Montemayor-1 core.

7. Conclusions

- 1 A detailed paleoenvironmental evolution of the lower Guadalquivir Basin during the Messinian has been proposed using benthic foraminifera from the Montemayor-1 core.
- 2 Relative sea-level fluctuations during the late Miocene-early Pliocene have been reconstructed using P/B ratio, depth marker species and a quantitative transfer function. A very sharp transgressive episode, changing from inner-middle shelf to middle slope settings, took place at the beginning of the studied deposits (latest Tortonian-earliest Messinian). After this maximum flooding, sea-level dropped, passing from the middle slope to the outer shelf. This sea-level fall appears to postdate the onset of the Messinian salinity crisis in the Mediterranean. Next, a progressive but slow sea level lowering occurred. Sea-level abruptly dropped close to the end of the Messinian. After a discontinuity close to the Miocene-Pliocene boundary, inner-middle shelf established during the early Pliocene. This transgressive-regressive sea-level trend is similar to that observed on the Atlantic side of the Rifian corridors. In the context of global fluctuating sea level, the continuous Messinian shallowing trend on the Betic and Rifian corridors is likely caused by regional tectonic uplift.

3 The distribution, composition, diversity and microhabitat preferences of the benthic foraminiferal assemblages of the late Miocene-early Pliocene in the lower Guadalquivir Basin are predominantly controlled by trophic conditions in terms of quantity and quality of the organic matter reaching the sea floor.

4 During the Messinian, the outer shelf fauna is characterised by relatively low diverse foraminiferal assemblages and dominance of epifaunal-shallow infaunal taxa. Similarly, the assemblages of the transitional interval between the upper slope and the outer shelf are low diverse and dominated by epifaunal-shallow infaunal taxa although epifaunal taxa are more important than on the outer shelf. Both the outer shelf and the transitional interval between the upper slope and the outer shelf faunas are consistent with a low organic matter input and high oxygen contents. The upper slope faunas are highly diverse and mainly dominated by shallow infaunal taxa indicating mesotrophic conditions with moderate oxygenation. The inner-middle shelf environments are characterized by a very low diverse fauna, dominated by intermediate infaunal and various deep infaunal taxa. Eutrophic conditions with very high organic matter supply and low oxygen concentrations are in agreement with this fauna.

5 Upwelling currents and river run-off are considered to be the major sources of organic matter at the study area. The sediments deposited in the upper slope are dominated by species from the *U. peregrina* s.l. assemblage that profit from pulses of labile marine organic matter related to upwelling events. The outer shelf has likely also been influenced by upwelling events indicated by the presence of *U. peregrina* s.l. and *B. spathulata*. The middle shelf muddy sediments may have been influenced by continental organic matter derived from river run-off. These

environments have been inhabited by *N. fabum* and *B. elongata* that can tolerate continental low quality organic matter.

Acknowledgements

We are very grateful to two anonymous reviewers for their constructive suggestions on an early version of the manuscript. This paper is part of the Research Projects CGL2010-20857 and CGL2009-11539/BTE of the Ministerio de Ciencia e Innovación of Spain, and the Research Group RNM-190 of the Junta de Andalucía. JNPA has been funded by a research scholarship provided by the Ministerio de Educación of Spain (F.P.U. scholarship).

References

- Aguirre, J., Sánchez-Almazo, I.M., 2004. The Messinian post-evaporitic deposits of the Gafares area (Almería-Níjar basin, SE Spain). A new view of the “Lago-Mare” facies. *Sedimentary Geology* 168, 71–95.
- Aguirre, J., Braga, J.C., Martín, J.M., 2007. El Mioceno marino del Prebético occidental (Cordillera Bética, SE de España): historia del cierre del Estrecho Norbético, in: Aguirre, J., Company, M., Rodríguez-Tovar, F.J. (Eds.), XIII Jornadas de la Sociedad Española de Paleontología: Guía de Excursiones. Instituto Geológico y Minero de España-Universidad de Granada, Granada, pp. 53–66.
- Aguirre, J., Castillo, C., Ferriz, F.J., Agustí, J., Oms, O., 1995. Marine-continental magnetobiostratigraphic correlation of the *Dolomys* subzone (middle of Late

- Ruscinian): implications for the Late Ruscinian age. *Palaeogeography, Palaeoclimatology, Palaeoecology* 117, 139–152.
- Arnold, A.J., Parker, W.C., 1999. Biogeography of planktonic Foraminifera, in: Sen Gupta, B.K. (Ed), *Modern Foraminifera*. Kluwer Academic Publishers, Dordrecht, pp. 103–122.
- Baceta, J.I., Pendón, J.G., 1999. Estratigrafía y arquitectura de facies de la Formación Niebla, Neógeno superior, sector occidental de la Cuenca del Guadalquivir. *Revista de la Sociedad Geológica de España* 12, 419–438.
- Báldi, K., Hohenegger J., 2008. Paleoecology of benthic foraminifera of Baden-Sooss section (Badenian, Middle Miocene, Vienna Basin, Austria). *Geologica Carpathica* 59, 411–424.
- Barbieri, R., 1998. Foraminiferal paleoecology at the Tortonian-Messinian boundary, Atlantic coast of northwestern Morocco. *Journal of Foraminiferal Research* 28, 102–123.
- Barbieri, R., Ori, G.G., 2000. Neogene palaeoenvironmental evolution in the Atlantic side of the Rifian Corridor (Morocco). *Palaeogeography, Palaeoclimatology, Palaeoecology* 163, 1–31.
- Barmawidjaja, D.M., Jorissen, F.J., Puskaric, S., van der Zwaan, G.J., 1992. Microhabitat selection by benthic foraminifera in the northern Adriatic Sea. *Journal of Foraminiferal Research* 22, 297–317.
- Benson, R.H., 1986. Messinian salinity crisis. *Encyclopedia of Earth System Science* 3, 161–167.
- Benson, R.H., Rakic-El Bied, K., Bonaduce, G., 1991. An important current reversal (influx) in the Rifian corridor (Morocco) at the Tortonian-Messinian Boundary: the end of Tethys ocean. *Paleoceanography* 6, 164–192.

- Berggren, W.A., Haq, B.U., 1976. The Andalusian Stage (Late Miocene): biostratigraphy, biochronology and palaeoecology. *Palaeogeography, Palaeoclimatology, Palaeoecology* 20, 67–129.
- Berggren, W.A., Benson, R.H., Haq, B.U., Riedel, W.R., Sanfilippo, A., Schrader, H.J., Tjalsma, R.C., 1976. The El Cuervo Section (Andalusia, Spain): micropaleontologic anatomy of an early Late Miocene lower bathyal deposit. *Marine Micropaleontology* 1, 195–247.
- Betzler, C., Braga, J.C., Martín, J.M., Sánchez-Almazo, I.M., Lindhorst, S., 2006. Closure of a seaway: Stratigraphic record and facies (Guadix basin, southern Spain). *International Journal of Earth Sciences (Geologische Rundschau)* 95, 903–910.
- Braga, J.C., Martín, J.M., Aguirre, J., 2002. Tertiary. Southern Spain, in: Gibbons, W., Moreno, T. (Eds.), *The Geology of Spain*. The Geological Society, London, pp 320–327.
- Braga, J.C., Martín, J.M., Riding, R., Aguirre, J., Sánchez-Almazo, I.M., Dinarès-Turell, J., 2006. Testing models for the Messinian salinity crisis: The Messinian record in Almería, SE Spain. *Sedimentary Geology* 188–189, 131–154.
- Braga, J.C., Martín, J.M., Aguirre, J., Baird, C.D., Grunnaleite, I., Jensen, N.B., Puga-Bernabéu, A., Saelen, G., Talbot, M.R., 2010. Middle-Miocene (Serravallian) temperate carbonates in a seaway connecting the Atlantic Ocean and the Mediterranean Sea (North Betic Strait, S Spain). *Sedimentary Geology* 225, 19–33.
- Civis, J., Sierro, F.J., González-Delgado, J.A., Flores, J.A., Andrés, I., de Porta, J., Valle, M.F., 1987. El Neógeno marino de la provincia de Huelva: Antecedentes y definición de las unidades litoestratigráficas, in: Civis, J. (Ed.), *Paleontología del Neógeno de Huelva*. Ediciones Universidad de Salamanca, Salamanca, pp. 9–21.

- Corbí, H. (2010). Los foraminíferos de la cuenca neógena del Bajo Segura (sureste de España). Bioestratigrafía y cambios paleoambientales en relación con la Crisis de Salinidad del Mediterráneo. PhD thesis, University of Alicante, Spain.
- Criado-Aldeanueva, F., García-Lafuente, J., Vargas, J.M., Del Río, J., Vázquez, A., Reul, A., Sánchez, A., 2006. Distribution and circulation of water masses in the Gulf of Cádiz from in situ observations. *Deep-Sea Research II* 53, 1144–1160.
- De Rijk, S., Jorissen, F.J., Rohling, E.J., Troelstra, S.R., 2000. Organic flux control on bathymetric zonation of Mediterranean benthic foraminifera. *Marine Micropaleontology* 40, 151–166.
- Diz, P., Francés, G., 2008. Distribution of live benthic foraminifera in the Ría de Vigo (NW Spain). *Marine Micropaleontology* 66, 165–191.
- Diz, P., Francés, G., Rosón, G., 2006. Effects of contrasting upwelling-downwelling on benthic foraminiferal distribution in the Ría de Vigo (NW Spain). *Journal of Marine Systems* 60, 1–18.
- Donnici, S., Serandrei Barbero, R., 2002. The benthic foraminiferal communities of the northern Adriatic continental shelf. *Marine Micropaleontology* 44, 93–123.
- Duchemin, G., Jorissen, F.J., Le Loc'h, F., Andrieux-Loyer, F., Hily, C., Thouzeau, G., 2008. Seasonal variability of living benthic foraminifera from the outer continental shelf of the Bay of Biscay. *Journal of Sea Research* 59, 297–319.
- Esteban, M., Braga, J.C., Martín, J.M., Santisteban, C., 1996. Western Mediterranean reef complexes, in: Franseen, E.K., Esteban, M., Ward, W.C., Rouchy, J.M. (Eds.), *Models for Carbonate Stratigraphy from Miocene Reef Complexes of Mediterranean Regions. Concepts in Sedimentology and Paleontology, Vol. 5. Society of Economic Paleontologists and Mineralogists, Tulsa, Oklahoma, pp. 55–72.*

- Fariduddin, M., Loubere, P., 1997. The surface ocean productivity response of deeper water benthic foraminifera in the Atlantic Ocean. *Marine Micropaleontology* 32, 289–310.
- Flores, J.A., 1987. El nanoplancton calcáreo en la formación «Arcillas de Gibraleón»: síntesis bioestratigráfica y paleoecológica, in: Civis, J. (Ed.), *Paleontología del Neógeno de Huelva*. Ediciones Universidad de Salamanca, Salamanca, pp. 65–68.
- Fontanier, C., Jorissen, F.J., Licari, L., Alexandre, A., Anschutz, P., Carbonel, P., 2002. Live benthic foraminiferal faunas from the Bay of Biscay: faunal density, composition, and microhabitats. *Deep-Sea Research I* 49, 751–785.
- Fontanier, C., Jorissen, F.J., Chaillou, G., David, C., Anschutz, P., Lafon, V., 2003. Seasonal and interannual variability of benthic foraminiferal faunas at 550 m depth in the Bay of Biscay. *Deep-Sea Research I* 50, 457–494.
- Galán, E., González, I., Mayoral, E., Vázquez, M. A., 1989. Caracterización y origen de la facies glauconítica de la Cuenca del Guadalquivir. *Estudios geológicos* 45, 169–175.
- Gautier, F., Clauzon, G., Suc, J.P., Cravatte, J., Violanti, D., 1994. Age et durée de la crise de la salinité messinienne. *Comptes Rendus de la Academie de la Sciences de Paris* 318, 1103–1109.
- Gebhardt, H., 1993. Neogene foraminifera from the Eastern Rabat area (Morocco): stratigraphy, palaeobathymetry and palaeoecology. *Journal of African Earth Sciences* 16, 445–464.
- Gebhardt, H., 1999. Middle to Upper Miocene benthonic foraminiferal palaeoecology of the Tap Marls (Alicante Province, SE Spain) and its palaeoceanographic implications. *Palaeogeography, Palaeoclimatology, Palaeoecology* 145, 141–156.

- Gläser, I., Betzler, C., 2002. Facies partitioning and sequence stratigraphy of cool-water, mixed carbonate-siliciclastic sediments (Upper Miocene Guadalquivir Domain, southern Spain). *International Journal of Earth Sciences (Geologische Rundschau)* 91, 1041–1053.
- Goineau, A., Fontanier, C., Jorissen, F.J., Lansard, B., Buscail, R., Mouret, A., Kerhervé, P., Zaragosi, S., Ernoult, E., Artéro, C., Anschutz, P., Metzger, E., Rabouille, C., 2011. Live (stained) benthic foraminifera from the Rhône prodelta (Gulf of Lion, NW Mediterranean): Environmental controls on a river-dominated shelf. *Journal of Sea Research* 65, 58–75.
- Gonzalez, R., Dias, J.M.A., Lobo, F., Mendes, I., 2004. Sedimentological and paleoenvironmental characterisation of transgressive sediments on the Guadiana Shelf (Northern Gulf of Cádiz, SW Iberia). *Quaternary International* 120, 133–144.
- González-Delgado, J.A., Civis, J., Dabrio, C.J., Goy, J.L., Ledesma, S., Pais, J., Sierro, F.J., Zazo, C., 2004. Cuenca del Guadalquivir, in: Vera, J.A. (Ed.), *Geología de España*. SGE-IGME, Madrid, pp. 543-550.
- González-Regalado, M.L., 1989. Estudio sistemático de los foraminíferos bentónicos de las arenas fosilíferas del Plioceno de Huelva: su significado paleoecológico. *Estudios Geológicos* 45, 101–119.
- González-Regalado, M.L., Ruiz, F., Tosquella, J., Baceta, J.I., Pendón, J.G., Abad, M., Hernández-Molina, F.J., Somoza, L., Díaz del Río, V., 2001. Foraminíferos bentónicos actuales de la plataforma continental del norte del Golfo de Cádiz. *Geogaceta* 29, 61–64.
- González-Regalado, M.L., Ruiz, F., Abad, M., Pendón, J.G., Tosquella, J., 2005. Los foraminíferos bentónicos del horizonte glauconítico inferior de la Formación

- <<Arcillas de Gibraleón>> (Depresión del Guadalquivir, SO España). *Geogaceta* 38, 127–130.
- González-Regalado, M.L., Ruiz, F., Abad, M., Civis, J., González-Delgado, J.A., Muñoz, J.M., García, E.X.M., Pendón, J.G., Toscano, A., 2009. Impact of storms on Pliocene benthic foraminiferal assemblages of southwestern Spain. *Ameghiniana* 46, 345–360.
- Gutiérrez-Mas, J.M., Hernández-Molina, F. J., López-Aguayo, F., 1996. Holocene sedimentary dynamics on the Iberian continental shelf of the Gulf of Cádiz (SW Spain). *Continental Shelf Research* 16, 1635–1653.
- Haq, B.U., Hardenbol, J., Vail, P.R., 1987. Chronology of fluctuating sea levels since the Triassic. *Science* 235, 1156–1167.
- Hardenbol, J., Thierry, J., Farley, M.B., Jaquin, T., de Graciansky, P., Vail, P.R. 1998. Mesozoic and Cenozoic sequence chronostratigraphic framework of European basins - chart 2: Cenozoic sequence chronostratigraphy, in: de Graciansky, P., Hardenbol, J., Jaquin, T., Vail, P.R. (Eds.), *Mesozoic and cenozoic sequence stratigraphy of european basins*. SEPM Special Publication, 60.
- Harris, L.C., Whiting, B.M., 2000. Sequence-stratigraphic significance of Miocene to Pliocene glauconite-rich layers, on- and offshore of the US Mid-Atlantic margin. *Sedimentary Geology* 134, 129–147.
- Haunold, T.G., Baal, C., Piller, W.E., 1997. Benthic foraminiferal associations in the Northern Bay of Safaga, Red Sea, Egypt. *Marine Micropaleontology* 29, 185–210.
- Hayek, L.A.C., Buzas, M.A., 1997. *Surveying Natural Populations*. Columbia University Press, New York.

- Hayward, B.W., Grenfell, H.R., Sabaa, A., Hayward, J.J., 2003. Recent benthic foraminifera from offshore Taranaki, New Zealand. *New Zealand Journal of Geology & Geophysics* 46, 489–518.
- Hodell, D.A., Benson, R.H., Kennett, J.P., Rakic-El Bied, K., 1989. Stable isotope stratigraphy of latest Miocene sequences in northwest Morocco: The Bou Regreg section. *Paleoceanography* 4, 467–482.
- Hodell, D.A., Benson, R.H., Kent, D.V., Boersma, A., Rakic-El Bied, K., 1994. Magnetostratigraphic, biostratigraphic, and stable isotope stratigraphy of an Upper Miocene drill core from the Salé Briqueterie (northwestern Morocco): A high-resolution chronology for the Messinian stage. *Paleoceanography* 9, 835–855.
- Hohenegger, J., 2005. Estimation of environmental paleogradient values based on presence/absence data: a case study using benthic foraminifera for paleodepth estimation. *Palaeogeography, Palaeoclimatology, Palaeoecology* 217, 115–130.
- Hohenegger, J., Andersen, N., Báldi, K., Ćorić, S., Pervesler, P., Rupp, C., Wagreich, M., 2008. Paleoenvironment of the Early Badenian (Middle Miocene) in the southern Vienna Basin (Austria)-multivariate analysis of the Baden-Soos section. *Geologica Carpathica* 59, 461–487.
- Hsü, K.J., Ryan, W.B.F., Cita, M.B., 1973. Late Miocene Desiccation of the Mediterranean. *Nature* 242, 240–244.
- Hsü, J.K., Montadert, L., Bernoulli, D., Cita, M.B., Erickson, A., Garrison, R.E., Kidd, R.B., Mélières, F., Müller, C., Wright, R., 1977. History of the Mediterranean salinity crisis. *Nature* 267, 1053–1078.
- Jorissen, F.J., 1988. Benthic foraminifera from the Adriatic Sea; Principles of phenotypic variation. *Utrecht Micropaleontology Bulletin* 37, 1–176.

- Jorissen, F.J., Barmawidjaja, D.M., Puskaric, S., van der Zwaan, G.J., 1992. Vertical distribution of benthic foraminifera in the northern Adriatic Sea: the relation with the organic flux. *Marine Micropaleontology* 19, 131–146.
- Jorissen, F.J., de Stigter, H.C., Widmark, J.G.V., 1995. A conceptual model explaining benthic foraminiferal microhabitats. *Marine Micropaleontology* 26, 3–15.
- Jorissen, F.J., Fontanier, C., Ellen, T., 2007. Paleoceanographical proxies based on deep-sea benthic foraminiferal assemblage characteristics, in: Hillaire-Marcel, C., De Vernal, A. (Eds.), *Developments in Marine Geology*, Vol. 1. Elsevier, Amsterdam, pp. 263–325.
- Kaiho, K., 1994. Benthic foraminiferal dissolved-oxygen index and dissolved-oxygen levels in the modern ocean. *Geology* 22, 719–722.
- Kaiho, K., 1999. Effect of organic carbon flux and dissolved oxygen on the benthic foraminiferal oxygen index (BFOI). *Marine Micropaleontology* 37, 67–76.
- Koho, K.A., García, R., de Stigter, H.C., Epping, E., Koning, E., Kouwenhoven, T.J., van der Zwaan, G.J., 2008. Sedimentary labile organic carbon and pore water redox control on species distribution of benthic foraminifera: A case study from Lisbon-Setúbal Canyon (southern Portugal). *Progress in Oceanography* 79, 55–82.
- Krijgsman, W., Hilgen, F.J., Raffi, I., Sierro, F.J. and Wilson, D.S., 1999a. Chronology, causes and progression of the Messinian salinity crisis. *Nature* 400, 652–655.
- Krijgsman, W., Langereis, C.G., Zachariasse, W.J., Boccaletti, M., Moratti, G., Gelati, R., Iaccarino, S., Papani, G., Villa, G., 1999b. Late Neogene evolution of the Taza-Guercif Basin (Rifian Corridor, Morocco) and implications for the Messinian salinity crisis. *Marine Geology* 153, 147–160.
- Krijgsman, W., Gaboardi, S., Hilgen, F.J., Iaccarino, S., de Kaenel, E., van der Laan, E., 2004. Revised astrochronology for the Ain el Beida section (Atlantic Morocco): No

- glacio-eustatic control for the onset of the Messinian Salinity Crisis. *Stratigraphy* 1, 87–101.
- Kucera, M., 2007. Planktonic foraminifera as tracers of past oceanic environments, in: Hillaire-Marcel, C., De Vernal, A. (Eds.), *Developments in Marine Geology*, Vol. 1. Elsevier, Amsterdam, pp. 213–262.
- Larrasoaña, J.C., González-Delgado, J.A., Civis, J., Sierro, F.J., Alonso-Gavilán, G., Pais, J., 2008. Magnetobiostratigraphic dating and environmental magnetism of Late Neogene marine sediments recovered at the Huelva-1 and Montemayor-1 boreholes (lower Guadalquivir basin, Spain). *Geo-Temas* 10, 1175–1178.
- Levin, L., Cage, J.D., 1998. Relationships between oxygen, organic matter and the diversity of bathyal macrofauna. *Deep-Sea Research II* 45, 129–163.
- Lourens, L.J., Hilgen, F.J., Shackleton, N.J., Laskar, J., Wilson, D.S., 2004. The Neogene Period, in: Gradstein F.M., Ogg J.G., Smith A.G., (Eds.), *A Geologic Time Scale 2004*. Cambridge University Press, Cambridge, pp. 409–440.
- Lutze, G.F., 1980. Depth distribution of benthic foraminifera on the continental margin off NW Africa. “Meteor” *Forschungs-Ergebnisse*, Part C, 32, 31–80.
- Lutze, G.F., Coulbourn, W.T., 1984. Recent benthic Foraminifera from the continental margin of northwest Africa: community structures and distribution. *Marine Micropaleontology* 8, 361–401.
- Lutze, G.F., Thiel, H., 1989. Epibenthic foraminifera from elevated microhabitats: *Cibicidoides wuellerstorfi* and *Planulina ariminensis*. *Journal of Foraminiferal Research* 19, 153–158.
- Maldonado, A., Somoza, L., Pallarés, L. 1999. The Betic orogen and the Iberian-African boundary in the Gulf of Cadiz: geological evolution (central North Atlantic). *Marine Geology* 155, 9–43.

- Malmgren, B.A., Haq, B.U., 1982. Assessment of quantitative techniques in paleobiogeography. *Marine Micropaleontology* 7, 213–230.
- Martín, J.M., Braga, J.C., 1994. Messinian events in the Sorbas basin in southeastern Spain and their implications in the recent history of the Mediterranean. *Sedimentary Geology* 90, 257–268.
- Martín, J.M., Braga, J.C., Betzler, C., 2001. The Messinian Guadalhorce corridor: The last northern, Atlantic-Mediterranean gateway. *Terra Nova* 13, 418–424.
- Martín, J.M., Braga, J.C., Aguirre, J., Puga-Bernabéu, A., 2009. History and evolution of the North-Betic Strait (Prebetic Zone, Betic Cordillera): A narrow, early Tortonian, tidal-dominated, Atlantic-Mediterranean marine passage. *Sedimentary Geology* 216, 80–90.
- Martín, J.M., Braga, J.C., Sánchez-Almazo, I.M., Aguirre, J., 2010. Temperate and tropical carbonate-sedimentation episodes in the Neogene Betic basins (S Spain) linked to climatic oscillations and changes in the Atlantic-Mediterranean connections. Constraints with isotopic data, in: Mutti, M., Piller, W., Betzler, C. (Eds.), *Carbonate Systems During the Oligocene-Miocene Climatic Transition*. International Association of Sedimentologists Special Publication, No. 42. Blackwell, Oxford. pp. 49–69.
- Martins, V., Jouanneau, J.-M., Weber, O., Rocha, F., 2006. Tracing the late Holocene evolution of the NW Iberian upwelling system. *Marine Micropaleontology* 59, 35–55.
- Mayoral, E., Pendón, J.G., 1987. Icnofacies y sedimentación en zona costera. Plioceno superior (?), litoral de Huelva. *Acta Geológica Hispánica* 21-22, 507–513.
- Melki, T., Kallel, N., Jorissen, F.J., Guichard, F., Dennielou, B., Berné, S., Labeyrie, L., Fontugne, M., 2009. Abrupt climate change, sea surface salinity and

- paleoproductivity in the western Mediterranean Sea (Gulf of Lion) during the last 28 kyr. *Palaeogeography, Palaeoclimatology, Palaeoecology* 279, 96–113.
- Mendes, I., Gonzalez, R., Dias, J.M.A., Lobo, F., Martins, V., 2004. Factors influencing recent benthic foraminifera distribution on the Guadiana shelf (Southwestern Iberia). *Marine Micropaleontology* 51, 171–192.
- Milker, Y., 2010. Western Mediterranean shelf foraminifera: Recent distribution, Holocene sea-level reconstructions, and paleoceanographic implications. PhD thesis, University of Hamburg, Germany.
- Milker, Y., Schmiedl, G., Betzler, C., Römer, M., Jaramillo-Vogel, D., Siccha, M., 2009. Distribution of recent benthic foraminifera in shelf carbonate environments of the Western Mediterranean Sea. *Marine Micropaleontology* 73, 207–225.
- Mojtahid, M., Griveaud, C., Fontanier, C., Anschutz, P., Jorissen, F.J., 2010a. Live benthic foraminiferal faunas along a bathymetrical transect (140–4800 m) in the Bay of Biscay (NE Atlantic). *Revue de Micropaléontologie* 53, 139–162.
- Mojtahid, M., Jorissen, F., Lansard, B., Fontanier, C., 2010b. Microhabitat selection of benthic foraminifera in sediments off the Rhône river mouth (NW Mediterranean). *Journal of Foraminiferal Research* 40, 231–246.
- Mojtahid, M., Jorissen, F., Lansard, B., Fontanier, C., Bombled, B., Rabouille, C., 2009. Spatial distribution of live benthic foraminifera in the Rhône prodelta: Faunal response to a continental-marine organic matter gradient. *Marine Micropaleontology* 70, 177–200.
- Mojtahid, M., Jorissen, F., Durrieu, J., Galgani, F., Howa H., Redois, F., Camps R. 2006. Benthic foraminifera as bio-indicators of drill cutting disposal in tropical east Atlantic outer shelf environments. *Marine Micropaleontology* 61, 58–75.

- Murray, J.W., 1991. Ecology and Palaeoecology of Benthic Foraminifera. Longman Scientific & Technical, UK.
- Murray, J.W., 2006. Ecology and Applications of Benthic Foraminifera. Cambridge University Press, Cambridge.
- Nelson, C.H., Baraza, J., Maldonado, A., Rodero, J., Escutia, C., Barber Jr., J.H. 1999. Influence of the Atlantic inflow and Mediterranean outflow currents on Late Quaternary sedimentary facies of the Gulf of Cádiz continental margin. *Marine Geology* 155, 99–129.
- Odin G.S., Matter, A. 1981. De glauconarium origine. *Sedimentology* 28, 611–641.
- Parker, F.L., 1954. Distribution of the Foraminifera in the northeastern Gulf of Mexico. *Bulletin of the Museum of Comparative Zoology* 111, 453–588.
- Pascual, A., Martínez-García, B., Rodríguez-Lázaro, J., Martín-Rubio, M., 2008. Distribución de los foraminíferos bentónicos en la plataforma marina de Vizcaya y Este de Cantabria. *Geogaceta* 44, 131–134.
- Perconig, E., 1973. El Andaluciense. XIII Coloquio Europeo de Micropaleontología. C. N. G. Enadimsa, Madrid, pp. 201–223.
- Perconig, E., Granados, L.F. 1973. El estratotipo del Andaluciense. XIII Coloquio Europeo de Micropaleontología. C. N. G. Enadimsa, Madrid, pp. 225–251.
- Pérez-Asensio, J.N., Aguirre, J., 2010. Benthic foraminiferal assemblages in temperate coral-bearing deposits from the Late Pliocene. *Journal of Foraminiferal Research* 40, 61–78.
- Retailleau, S., Howa, H., Schiebel, R., Lombard, F., Eynaud, F., Schmidt, S., Jorissen, F., Labeyrie, L., 2009. Planktic foraminiferal production along an offshore-onshore transect in the south-eastern Bay of Biscay. *Continental Shelf Research* 29, 1123–1135.

- Rezqi, H., Oujidi, M., Boutakiout, M., Labraimi, M., 2000. Analyse quantitative des foraminifères benthiques actuels de la marge atlantique marocaine entre Cap Drâa et Cap Juby: reponses fauniques aux changements de l'environnement. *Journal of African Earth Sciences* 30, 375–400.
- Riaza, C., Martínez del Olmo, W., 1996. Depositional model of the Guadalquivir-Gulf of Cádiz Tertiary basin, in: Friend, P., Dabrio, C.J., (Eds.), *Tertiary basins of Spain*. Cambridge University Press, Cambridge, pp. 330–338.
- Riding, R., Braga, J.C., Martín, J.M., Sánchez-Almazo, I.M., 1998. Mediterranean Messinian Salinity Crisis: constraints from a coeval marginal basin, Sorbas, southeastern Spain. *Marine Geology* 146, 1–20.
- Roldán, F.J., 1995. Evolución neógena de la Cuenca del Guadalquivir. Ph.D. Thesis, University of Granada, Spain.
- Roveri, M., Manzi, V., 2006. The Messinian salinity crisis: looking for a new paradigm?. *Palaeogeography, Palaeoclimatology, Palaeoecology* 238, 386–398.
- Sanz de Galdeano, C., 1990. Geologic evolution of the Betic Cordilleras in the Western Mediterranean, Miocene to the present. *Tectonophysics* 172, 107–119.
- Sanz de Galdeano, C., Vera, J.A., 1992. Stratigraphic record and palaeogeographical context of the Neogene basins in the Betic Cordillera, Spain. *Basin Research* 4, 21–36.
- Sarnthein, M., Thiede, J., Pflaumann, U., Erlenkeuser, H., Fütterer, D., Koopmann, B., Lange, H., Seibold, E., 1982. Atmospheric and oceanic circulation patterns off northwest Africa during the past 25 million years, in: Von Rad, U., Hinz, K., Sarnthein, M., Seibold, E. (Eds). *Geology of the Northwest Africa continental margin*. Springer-Verlag, New York, pp. 545–604.

- Schmiedl, G., Mackensen, A., Müller, P.J., 1997. Recent benthic foraminifera from the eastern South Atlantic Ocean: Dependence on food supply and water masses. *Marine Micropaleontology* 32, 249–287.
- Schmiedl, G., de Bovée, F., Buscail, R., Charrière, B., Hemleben, C., Medernach, L., Picon, P., 2000. Trophic control of benthic foraminiferal abundance and microhabitat in the bathyal Gulf of Lions, western Mediterranean Sea. *Marine Micropaleontology* 40, 167–188.
- Schmiedl, G., Mitschele, A., Beck, S., Emeis, K.-C., Hemleben, C., Schulz, H., Sperling, M., Weldeab, S., 2003. Benthic foraminiferal record of ecosystem variability in the eastern Mediterranean Sea during times of sapropel S5 and S6 deposition. *Palaeogeography, Palaeoclimatology, Palaeoecology* 190, 139–164.
- Schmiedl, G., Kuhnt, T., Ehrmann, W., Emeis, K.-C., Hamann, Y., Kotthoff, U., Dulski, P., Pross, J., 2010. Climatic forcing of eastern Mediterranean deep-water and benthic ecosystems during the past 22 000 years. *Quaternary Science Reviews* 29, 3006–3020.
- Schönfeld, J., 1997. The impact of the Mediterranean Outflow Water (MOW) on Benthic foraminiferal assemblages and surface sediments at the southern Portuguese continental margin. *Marine Micropaleontology* 29, 211–236.
- Schönfeld, J., 2002. Recent benthic foraminiferal assemblages in deep high-energy environments from the Gulf of Cadiz (Spain). *Marine Micropaleontology* 44, 141–162.
- Schönfeld, J., 2006. Taxonomy and distribution of the *Uvigerina peregrina* plexus in the tropical to northeastern Atlantic. *Journal of Foraminiferal Research* 36, 355–367.

- Schönfeld, J., Altenbach, A.V., 2005. Late Glacial to Recent distribution pattern of deep-water *Uvigerina* species in the northeastern Atlantic: Marine Micropaleontology 57, 1–24.
- Sgarrella, F., Moncharmont Zei, M., 1993. Benthic foraminifera in the Gulf of Naples (Italy): systematics and autoecology. Bollettino della Società Paleontologica Italiana 32, 145–264.
- Shackleton, N.J., Hall, M.A., Pate, D., 1995. Pliocene stable isotope stratigraphy of site 846. Proceedings of the Ocean Drilling Program, Scientific Results 138, 337–355.
- Sierro, F.J., 1985. Estudio de los foraminíferos planctónicos, bioestratigrafía y cronoestratigrafía del Mio-Plioceno del borde occidental de la cuenca del Guadalquivir (S.O. de España). Stvdia Geologica Salmanticensia 21, 7–85.
- Sierro, F.J., 1987. Foraminíferos planctónicos del Neógeno marino del sector occidental de la cuenca del Guadalquivir: síntesis y principales resultados, in: Civis, J. (Ed.), Paleontología del Neógeno de Huelva. Ediciones Universidad de Salamanca, Salamanca, pp. 23–54.
- Sierro, F.J., Flores, J.A., 1992. Evolución de las fosas bética y rifeña y la comunicación Atlántico-Mediterráneo durante el Mioceno. Simposios del III Congreso Geológico de España y VIII Congreso Latinoamericano de Geología 2, 563–567.
- Sierro, F.J., Flores, J.A., Civis, J., González-Delgado, J.A., Francés, G., 1993. Late Miocene globorotaliid event-stratigraphy and biogeography in the NE-Atlantic and Mediterranean. Marine Micropaleontology 21, 143–168.
- Sierro, F.J., González-Delgado, J.A., Dabrio, C.J., Flores, J.A., Civis, J., 1996. Late Neogene depositional sequences in the foreland basin of Guadalquivir (SW Spain), in: Friend, P., Dabrio, C.J. (Eds.), Tertiary basins of Spain. Cambridge University Press, Cambridge, pp. 339–345.

- Soria, J.M., Fernández, J. and Viseras, C., 1999. Late Miocene stratigraphy and palaeogeographic evolution of the intramontane Guadix Basin (central Betic Cordillera, Spain): implications for an Atlantic-Mediterranean connection. *Palaeogeography, Palaeoclimatology, Palaeoecology* 151, 255–266.
- Spezzaferri, S., Tamburini, F., 2007. Paleodepth variations on the Eratosthenes Seamount (Eastern Mediterranean): sea-level changes or subsidence?. *eEarth Discussions* 2, 115–132.
- Stefanelli, S., 2004. Cyclic changes in oxygenation based on foraminiferal microhabitats: Early-Middle Pleistocene, Lucania Basin (southern Italy). *Journal of Micropalaeontology* 23, 81–95.
- Takata, H., Nomura, R., Khim, B.-K., 2010. Response of abyssal benthic foraminifera to mid-Oligocene glacial events in the eastern Equatorial Pacific Ocean (ODP Leg 199). *Palaeogeography, Palaeoclimatology, Palaeoecology* 292, 1–11.
- Van der Zwaan, G.J. and Jorissen, F.J., 1991. Biofacial patterns in river-induced shelf anoxia, in: Tyson, R.V., Pearson, T.H. (Eds), *Modern and Ancient Continental Shelf Anoxia*. Geological Society, Special Publication 58, London, pp. 65–82.
- Van Hinsbergen, D.J.J., Kouwenhoven, T.J., van der Zwaan, G.J., 2005. Paleobathymetry in the backstripping procedure: Correction for oxygenation effects on depth estimates. *Palaeogeography, Palaeoclimatology, Palaeoecology* 221, 245–265.
- Van Marle, L.J., 1988. Bathymetric distribution of benthic foraminifera on the Australian-Irian Jaya continental margin, eastern Indonesia. *Marine Micropaleontology* 13, 97–152.

- Van Morkhoven, F.P.C.M., Berggren, W.A., Edwards, A.S., 1986. Cenozoic Cosmopolitan Deep-water Benthic Foraminifera. Bulletin des Centres de Recherches Exploration-Production Elf-Aquitaine, Mémoire 11, Pau.
- Vargas, J.M., García-Lafuente, J., Delgado, J., Criado, F., 2003. Seasonal and wind-induced variability of Sea Surface Temperature patterns in the Gulf of Cádiz. *Journal of Marine Systems* 38, 205–219.
- Viguié, C., 1974. Le Néogène de l'Andalousie Nord-occidentale (Espagne). Histoire Géologique du «Bassin du Bas Guadalquivir». Ph.D. Thesis, University of Bordeaux, France.
- Villanueva-Guimerans, P., Canudo, I., 2008. Assemblages of recent benthic foraminifera from the northeastern Gulf of Cádiz. *Geogaceta* 44, 139–142.
- Zonneveld, K.A.F., Versteegh, G.J.M., Kasten, S., Eglinton, T.I., Emeis, K.-C., Huguet, C., Koch, B.P., de Lange, G.J., de Leeuw, J.W., Middelburg, J.J., Mollenhauer, G., Prahl, F.G., Rethemeyer, J., Wakeham, S.G., 2010. Selective preservation of organic matter in marine environments; processes and impact on the sedimentary record. *Biogeosciences* 7, 483–511.

Figure captions

Fig. 1. Geological map of the Betic Cordillera showing the Guadalquivir foreland basin (modified from Martín et al., 2010). The inset is shown in figure 2.

Fig. 2. Geological map of the lower Guadalquivir Basin including Montemayor-1 core location (modified from Civis et al., 1987).

Fig. 3. Log of the Montemayor-1 core and magnetobiostratigraphic framework.

Magnetostratigraphy follows the ATNTS2004 (Lourens et al., 2004). Biostratigraphy is based on the planktonic foraminifera events (PF events) of Sierro et al. (1993) and first occurrence of *Globorotalia puncticulata*. Numbers in the right-hand side column are sedimentation rates (cm/kyr) estimated for the Montemayor-1 core.

Fig. 4. Curves showing the planktonic-benthonic ratio (P/B ratio), sand content, and number of benthic foraminiferal per gram of sediment (N/g) along the Montemayor-1 core.

Fig. 5. Number of taxa, diversity metrics (Shannon index H, evenness E) and dominance.

Fig. 6. Some of the most abundant and representative benthic foraminiferal species in the Montemayor-1 core. A) *Cibicidoides pachyderma*, spiral side; B) *Cibicidoides pachyderma*, peripheral view; C) *Cibicidoides floridanus*, spiral side; D) *Brizalina spathulata*, side view; E) *Nonion fabum*, side view; F) *Nonion fabum*, peripheral view;

G) *Ammonia beccarii*, spiral side; H) *Bulimina elongata*, side view; I) *Uvigerina peregrina* s.l., side view; J) *Bulimina subulata*, side view; K) *Planulina ariminensis*, spiral side; L) *Valvulineria complanata*, spiral side; M) *Valvulineria complanata*, peripheral view; N) *Cassidulina laevigata*, apertural side; O) *Anomalinoidea flinti*, spiral side; P) *Siphonina reticulata*, side view; Q) *Oridorsalis umbonatus*, spiral side; R) *Uvigerina striatissima*, side view; S) *Hanzawaia boueana*, umbilical side. Scale bars = 100 μm .

Fig. 7. Benthic foraminiferal assemblages as derived from Q-mode Principal Component Analyses (PCA). Principal component loadings higher than 0.5 are considered significant following the suggestions of Malmgren and Haq (1982) and indicated by gray shading.

Fig. 8. Relative abundance (in percentage) of dominant taxa as extracted from the Q-mode benthic foraminiferal assemblages.

Fig. 9. Benthic foraminiferal assemblages as derived from R-mode Principal Component Analyses (PCA). Significant principal component scores are indicated in gray.

Fig. 10. Estimated paleodepth changes for the Montmayor-1 core. Horizontal bars represent the 95% confidence intervals. Three important sea-level drops are shown at 211.5, 176.5, and 61.5 m. This sea-level trend is correlated with that inferred in the Rifian corridors by Barbieri and Ori (2000) and with the global sea-level curve of Hardenbol et al. (1998). The two last shallowing events correlates precisely with similar

lowering inferred in the Rifian corridors. The sea-level fall at about 211.5 m can be linked with the onset of the MSC.

Fig. 11. Distribution of microhabitat preferences of benthic foraminifera (in percentage of the total taxa) along the studied section.

ACCEPTED MANUSCRIPT

Table captions

Table 1. Depth ranges of the benthic foraminifera from the Montemayor-1 core. Minimum, maximum, average depth and standard deviation (SD) are indicated. Bathymetric ranges are based on Berggren and Haq (1976), Berggren et al. (1976), Lutze (1980), van Morkhoven et al. (1986), van Marle (1988), González-Regalado (1989), Sgarrella and Moncharmont Zei (1993), Schönfeld (1997), González-Regalado et al. (2001), Murray (2006), Schönfeld (2006), Spezzaferrri and Tamburini (2007), Pascual et al. (2008), Villanueva-Guimerans and Canudo (2008), González-Regalado et al. (2009), and Corbí (2010).

Table 2. Paleodepth estimates in meters, and lower and upper confidence limits (CL).

Table 3. Microhabitat preferences of benthic foraminifera from the Montemayor-1 core.

Table 4. Pearson correlation coefficients at p -value < 0.01 of the Q-mode and R-mode PCA assemblages and the other measured parameters.

Table 5. Results of the Q-mode principal component analysis with indication of the more representative benthic foraminiferal species.

Table 6. Results of the R-mode principal component assemblages with indication of the more representative benthic foraminiferal species.

Table 1.

Species	Minimum depth	Maximum depth	Average depth	SD
<i>Ammonia beccarii</i>	0	100	50	50.00
<i>Ammonia inflata</i>	20	30	25	5.00
<i>Ammonia</i> sp.	0	100	50	50.00
<i>Amphicoryna</i> sp.	9	2860	1434.5	1425.50
<i>Anomalinoidea flinti</i>	600	2000	1300	700.00
<i>Bolivina punctata</i>	50	2000	1025	975.00
<i>Brizalina dilatata</i>	15	3000	1507.5	1492.50
<i>Brizalina spathulata</i>	30	3547	1788.5	1758.50
<i>Brizalina</i> sp.	15	3547	1781	1766.00
<i>Bulimina aculeata</i>	5	4000	2002.5	1997.50
<i>Bulimina costata</i>	50	3241	1645.5	1595.50
<i>Bulimina elongata</i>	16	200	108	92.00
<i>Bulimina mexicana</i>	100	2000	1050	950.00
<i>Bulimina</i> sp.	5	4000	2002.5	1997.50
<i>Cassidulina laevigata</i>	30	2500	1265	1235.00
<i>Cassidulina</i> sp.	30	3588	1809	1779.00
<i>Cibicides</i> sp.	0	2000	1000	1000.00
<i>Cibicidoides dutemplei</i>	100	600	350	250.00
<i>Cibicidoides floridanus</i>	100	200	150	50.00
<i>Cibicidoides pachyderma</i>	30	4000	2015	1985.00
<i>Cibicidoides ungerianus</i>	50	4000	2025	1975.00
<i>Cibicidoides</i> sp.	30	4000	2015	1985.00
<i>Fursenkoina schreibersiana</i>	20	200	110	90.00
<i>Globocassidulina subglobosa</i>	50	4000	2025	1975.00
<i>Gyroidinoides soldanii</i>	100	5000	2550	2450.00
<i>Gyroidinoides umbonatus</i>	16	2000	1008	992.00
<i>Hanzawaia boueana</i>	30	200	115	85.00
<i>Hoeglundina elegans</i>	30	4330	2180	2150.00
<i>Lagena</i> sp.	16	3500	1758	1742.00
<i>Lenticulina</i> sp.	19	4500	2259.5	2240.50
<i>Marginulina costata</i>	50	310	180	130.00
<i>Martinottiella communis</i>	200	3000	1600	1400.00
<i>Melonis barleeianum</i>	13	3974	1993.5	1980.50
<i>Melonis soldanii</i>	90	1000	545	455.00
<i>Melonis</i> sp.	13	4800	2406.5	2393.50
<i>Nonion fabum</i>	12	200	106	94.00
<i>Oridorsalis umbonatus</i>	65	4000	2032.5	1967.50
<i>Orthomorphina tenuicostata</i>	50	1000	525	475.00
<i>Planulina ariminensis</i>	70	1300	685	615.00
<i>Planulina</i> sp.	70	4700	2385	2315.00
<i>Pullenia bulloides</i>	60	4000	2030	1970.00
<i>Siphonina reticulata</i>	55	1500	777.5	722.50
<i>Siphotextularia concava</i>	50	631	340.5	290.50
<i>Sphaeroidina bulloides</i>	25	4500	2262.5	2237.50
<i>Stilostomella monilis</i>	100	2500	1300	1200.00
<i>Textularia</i> sp.	0	2000	1000	1000.00

<i>Trifarina bradyi</i>	0	600	300	300.00
<i>Uvigerina canariensis</i>	150	1097	623.5	473.50
<i>Uvigerina peregrina</i> s.l.	100	4400	2250	2150.00
<i>Uvigerina striatissima</i>	200	2000	1100	900.00
<i>Valvulineria complanata</i>	30	100	65	35.00

ACCEPTED MANUSCRIPT

Table 2.

Core depth (m)	Paleodepth (m)	Lower CL	Upper CL
256.50	31.88	-25.32	89.08
254.00	449.67	301.18	598.16
251.50	394.53	239.99	549.08
249.00	383.67	244.64	522.69
246.50	321.86	210.09	433.63
244.00	447.91	313.78	582.05
241.50	443.72	295.62	591.81
239.00	383.02	251.29	514.75
236.50	440.75	283.07	598.43
234.00	458.48	317.39	599.57
231.50	401.62	298.15	505.10
229.00	370.43	231.37	509.48
227.00	439.12	298.50	579.75
224.00	342.36	222.61	462.11
221.50	372.87	234.63	511.10
219.00	405.48	275.03	535.93
216.50	405.27	230.55	580.00
214.00	383.92	218.85	548.98
211.50	156.63	48.45	264.81
209.00	247.46	121.20	373.71
206.50	303.18	186.51	419.85
204.00	339.13	192.95	485.31
201.50	341.18	230.76	451.60
199.50	375.50	248.36	502.64
196.50	333.72	216.86	450.58
194.00	334.10	224.06	444.13
191.50	326.20	175.12	477.27
189.00	307.78	180.57	434.99
186.50	269.44	166.35	372.54
184.00	301.41	171.45	431.36
181.50	287.80	162.02	413.58
179.00	282.82	165.26	400.39
176.50	113.74	25.65	201.83
174.00	182.35	123.74	240.96
171.50	166.25	72.89	259.61
169.00	197.67	117.59	277.74
166.50	166.83	105.78	227.88
164.00	167.09	106.56	227.63
161.50	161.61	99.03	224.19
159.00	189.16	109.18	269.14
157.00	161.68	102.72	220.65
154.00	164.57	100.07	229.07
151.50	155.43	92.55	218.30
149.00	155.08	105.60	204.55
146.50	171.87	111.02	232.72
144.00	162.91	106.42	219.40
141.50	214.61	140.83	288.39
139.00	162.52	102.45	222.58

136.50	179.19	117.94	240.44
134.00	173.87	112.11	235.63
131.50	168.71	106.75	230.67
129.00	190.47	128.67	252.27
126.50	179.28	119.27	239.29
124.00	230.78	160.65	300.90
121.50	175.32	119.02	231.62
119.00	176.16	120.81	231.51
116.50	166.96	111.89	222.03
114.00	194.59	127.54	261.65
112.50	181.35	124.82	237.87
109.00	168.79	107.86	229.72
106.50	186.27	118.63	253.90
104.00	183.70	123.02	244.38
101.50	170.59	113.55	227.64
99.00	167.50	105.51	229.50
96.50	151.64	95.13	208.15
94.00	175.42	114.56	236.27
91.50	165.42	102.85	227.99
88.50	180.08	120.27	239.89
86.50	145.96	90.01	201.91
84.00	170.39	97.52	243.25
81.50	142.10	86.03	198.17
79.00	149.95	102.74	197.17
76.50	155.04	96.88	213.21
74.50	160.35	101.69	219.02
71.50	149.16	92.25	206.07
69.00	148.26	92.60	203.93
66.50	134.91	81.70	188.12
64.50	37.94	-14.25	90.13
61.50	46.80	15.50	78.09
59.00	47.83	20.87	74.78
56.50	52.97	0.84	105.11
54.00	44.27	2.30	86.25
51.50	48.18	0.29	96.06
49.00	40.04	-1.01	81.09
46.50	49.58	4.65	94.51
44.00	40.99	4.73	77.25
41.50	52.68	23.16	82.19
39.00	12.37	-27.85	52.60
36.50	13.26	-11.84	38.36

Table 3.

Microhabitat				
Epifauna	Epifauna-shallow infauna	Shallow infauna	Intermediate infauna	Deep infauna
<i>Asterigerinata mamilla</i>	<i>Ammonia beccarii</i>	<i>Amphicoryna scalaris</i>	<i>Melonis barleeaanum</i>	<i>Cassidulinoides bradyi</i>
<i>Asterigerinata</i> sp.	<i>Ammonia inflata</i>	<i>Amphicoryna semicostata</i>	<i>Melonis soldanii</i>	<i>Fursenkoina schreibersiana</i>
<i>Cibicides refulgens</i>	<i>Ammonia tepida</i>	<i>Amphicoryna sublineata</i>	<i>Melonis</i> sp.	<i>Globobulimina affinis</i>
<i>Cibicides lobatulus</i>	<i>Ammonia</i> sp.	<i>Amphicoryna</i> sp.	<i>Nonion boueanum</i>	<i>Globobulimina ovula</i>
<i>Cibicides wuellerstorfi</i>	<i>Anomalinoidea flinti</i>	<i>Bigenerina nodosaria</i>	<i>Nonionella turgida</i>	<i>Globobulimina</i> sp.
<i>Cibicides</i> sp.	<i>Anomalinoidea helacinus</i>	<i>Bolivina punctata</i>	<i>Nonionella</i> sp.	<i>Pleurostomella</i> sp.
<i>Cymbaloporeta squamosa</i>	<i>Anomalinoidea</i> sp.	<i>Bolivina reticulata</i>	<i>Rectuvigerina</i> sp.	<i>Praeglobobulimina ovata</i>
<i>Discorbis</i> sp.	<i>Burseolina calabra</i>	<i>Bolivina</i> sp.		
<i>Elphidium advenum</i>	<i>Cassidulina crassa</i>	<i>Brizalina arta</i>		
<i>Elphidium complanatum</i>	<i>Cassidulina</i> sp. 1	<i>Brizalina dilatata</i>		
<i>Elphidium macellum</i>	<i>Cassidulina</i> sp.	<i>Brizalina spathulata</i>		
<i>Hanzawaia boueana</i>	<i>Cibicidoides dutemplei</i>	<i>Brizalina</i> sp.		
<i>Hanzawaia</i> sp.	<i>Cibicidoides floridanus</i>	<i>Bulimina aculeata</i>		
<i>Planulina ariminensis</i>	<i>Cibicidoides incrassatus</i>	<i>Bulimina alazanensis</i>		
<i>Planulina</i> sp.	<i>Cibicidoides kullenbergi</i>	<i>Bulimina costata</i>		
<i>Rosalina</i> sp.	<i>Cibicidoides pachyderma</i>	<i>Bulimina elongata</i>		
	<i>Cibicidoides ungerianus</i>	<i>Bulimina mexicana</i>		
	<i>Cibicidoides</i> sp.	<i>Bulimina subulata</i>		
	<i>Elphidium</i> sp.	<i>Bulimina</i> sp.		
	<i>Eponides</i> sp.	<i>Cancris auriculus</i>		
	<i>Fissurina</i> sp.	<i>Cancris</i> sp.		
	<i>Globocassidulina subglobosa</i>	<i>Cassidulina carinata</i>		
	<i>Gyroidinoides laevigatus</i>	<i>Cassidulina laevigata</i>		
	<i>Gyroidinoides soldanii</i> s.l.	<i>Chrysalogonium</i> sp.		
	<i>Gyroidinoides umbonatus</i>	<i>Dentalina leguminiformis</i>		
	<i>Gyroidinoides</i> sp.	<i>Dentalina</i> sp.		
	<i>Heterolepa bellincionii</i>	<i>Dorothia gibbosa</i>		
	<i>Hoeglundina elegans</i>	<i>Eggerella bradyi</i>		
	<i>Lagena striata</i>	<i>Florilus</i> sp.		

<i>Lagena</i> sp.	<i>Glandulina</i> sp.
<i>Lenticulina calcar</i>	<i>Globulina</i> sp.
<i>Lenticulina cultrata</i>	<i>Martinottiella communis</i>
<i>Lenticulina curvisepta</i>	<i>Nodosarella</i> sp.
<i>Lenticulina inornata</i>	<i>Nodosaria pentecostata</i>
<i>Lenticulina rotulata</i>	<i>Nodosaria</i> sp.
<i>Lenticulina vortex</i>	<i>Nonion</i> sp.
<i>Lenticulina</i> sp.	<i>Orthomorphina tenuicostata</i>
<i>Marginulina costata</i>	<i>Orthomorphina</i> sp.
<i>Marginulina glabra</i>	<i>Pandaglandulina dinapolii</i>
<i>Marginulina hirsuta</i>	<i>Pullenia bulloides</i>
<i>Marginulina</i> sp.	<i>Pullenia quinqueloba</i>
<i>Neoeponides</i> sp. 1	<i>Pullenia salisburyi</i>
<i>Oridorsalis umbonatus</i>	<i>Reussella spinulosa</i>
<i>Planularia</i> sp.	<i>Stilostomella monilis</i>
<i>Quinqueloculina</i> sp.	<i>Stilostomella vertebralis</i>
<i>Siphonina reticulata</i>	<i>Stilostomella</i> sp. 1
<i>Siphotextularia concava</i>	<i>Stilostomella</i> sp.
<i>Sphaeroidina bulloides</i>	<i>Trifarina angulosa</i>
<i>Spiroplectinella sagittula</i>	<i>Trifarina bradyi</i>
<i>Textularia agglutinans</i>	<i>Uvigerina canariensis</i>
<i>Textularia calva</i>	<i>Uvigerina peregrina</i> s.l.
<i>Textularia pala</i>	<i>Uvigerina rutila</i>
<i>Textularia pseudorugosa</i>	<i>Uvigerina striatissima</i>
<i>Textularia</i> sp.	<i>Valvulineria complanata</i>
<i>Vaginulina</i> sp.	<i>Valvulineria</i> sp.

Table 4.

	QPC1	QPC2	QPC3	RPC1	RPC2	RPC3	P/B ratio	% sand	N/g	Number of taxa	H	E	D
QPC1	1.000												
QPC2	-0.674	1.000											
QPC3		-0.643	1.000										
RPC1		0.318	-0.753	1.000									
RPC2		-0.492	0.472		1.000								
RPC3	0.848	-0.575				1.000							
P/B ratio		-0.483	0.655		0.816		1.000						
% sand	-0.529	0.552	-0.428	0.372		0.488		1.000					
N/g	-0.283	0.311							1.000				
Number of taxa	0.392	-0.571	0.294		0.317	0.415	0.374			1.000			
H	0.481	-0.567				0.553				0.787	1.000		
E	0.356	-0.314				0.498				0.358	0.828	1.000	
D		0.458			-0.324	-0.316	-0.313			-0.567	-0.880	-0.822	1.000

PC assemblage	Variance (%)	Species	Score
1	49.6	<i>Cibicidoides pachyderma</i>	6.86
		<i>Cibicidoides</i> sp.	1.98
		<i>Cibicidoides floridanus</i>	1.22
		<i>Brizalina spathulata</i>	1.03
2	8.5	<i>Nonion fabum</i>	7.20
		<i>Ammonia beccarii</i>	2.01
		<i>Spiroplectinella</i> sp.	1.31
		<i>Ammonia</i> sp.	1.19
		<i>Bulimina elongata</i>	1.13
		<i>Brizalina spathulata</i>	1.05
3	23.7	<i>Uvigerina peregrina</i> s.l.	6.01
		<i>Bulimina subulata</i>	2.65
		<i>Cibicidoides pachyderma</i>	2.46
		<i>Planulina ariminensis</i>	1.77
		<i>Cibicidoides</i> sp.	1.22

Table 5.

PC assemblage	Variance (%)	Species	Loading
1	11.5	<i>Spiroplectinella</i> sp.	0.85
		<i>Valvulineria complanata</i>	0.76
		<i>Textularia</i> sp.)	0.70
		<i>Orthomorphina tenuicostata</i>	0.68
		<i>Melonis barleeanum</i>	0.68
		<i>Textularia agglutinans</i>	0.67
		<i>Cassidulina laevigata</i>	0.66
		<i>Ammonia beccarii</i>	0.56
		2	9.9
<i>Cibicidoides incrassatus</i>	-0.67		
<i>Uvigerina canariensis</i>	-0.65		
<i>Globocassidulina subglobosa</i>	-0.60		
<i>Planulina</i> sp.	-0.59		
<i>Siphonina reticulata</i>	-0.58		
<i>Oridorsalis umbonatus</i>	-0.57		
<i>Uvigerina striatissima</i>	-0.56		
<i>Planulina ariminensis</i>	-0.55		
<i>Gyroidinoides</i> sp.	-0.54		
<i>Anomalinoidea</i> sp.	-0.53		
3	9.7		
		<i>Cibicidoides floridanus</i>	0.60
		<i>Pullenia bulloides</i>	0.59
		<i>Sphaeroidina bulloides</i>	0.55
		<i>Lenticulina</i> sp.	0.55
		<i>Hanzawaia boueana</i>	0.53
		<i>Melonis soldanii</i>	0.53

	<i>Gyroidinoides soldanii</i>	0.51
--	-------------------------------	------

Table 6.

ACCEPTED MANUSCRIPT

Highlights

> We study Messinian benthic foraminifera from the lower Guadalquivir Basin. > Paleodepth analyses show a transgressive-regressive cycle from the bottom to the top. > Trophic conditions and bottom oxygenation controlled the assemblages. > Similar paleoenvironmental evolution is observed in NW Morocco. > Tectonic and sea-level evolution that led the Messinian salinity crisis is analyzed.

Figure 1

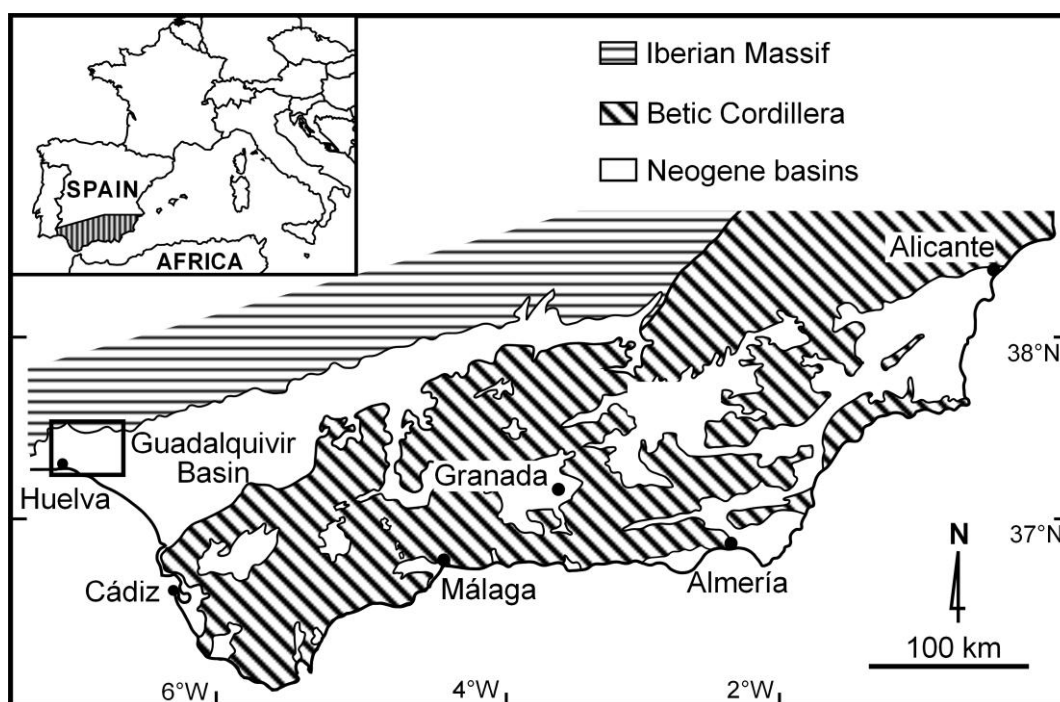


Figure 2

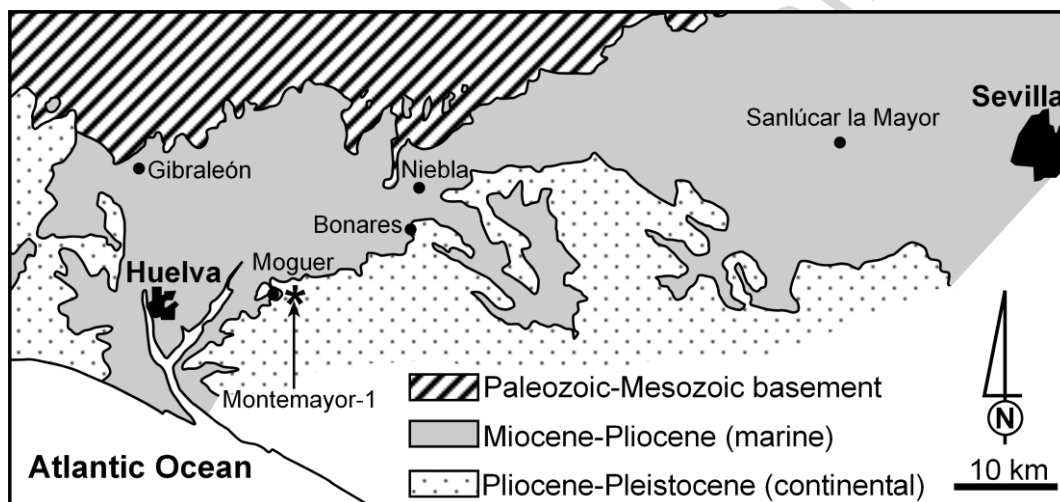


Figure 3

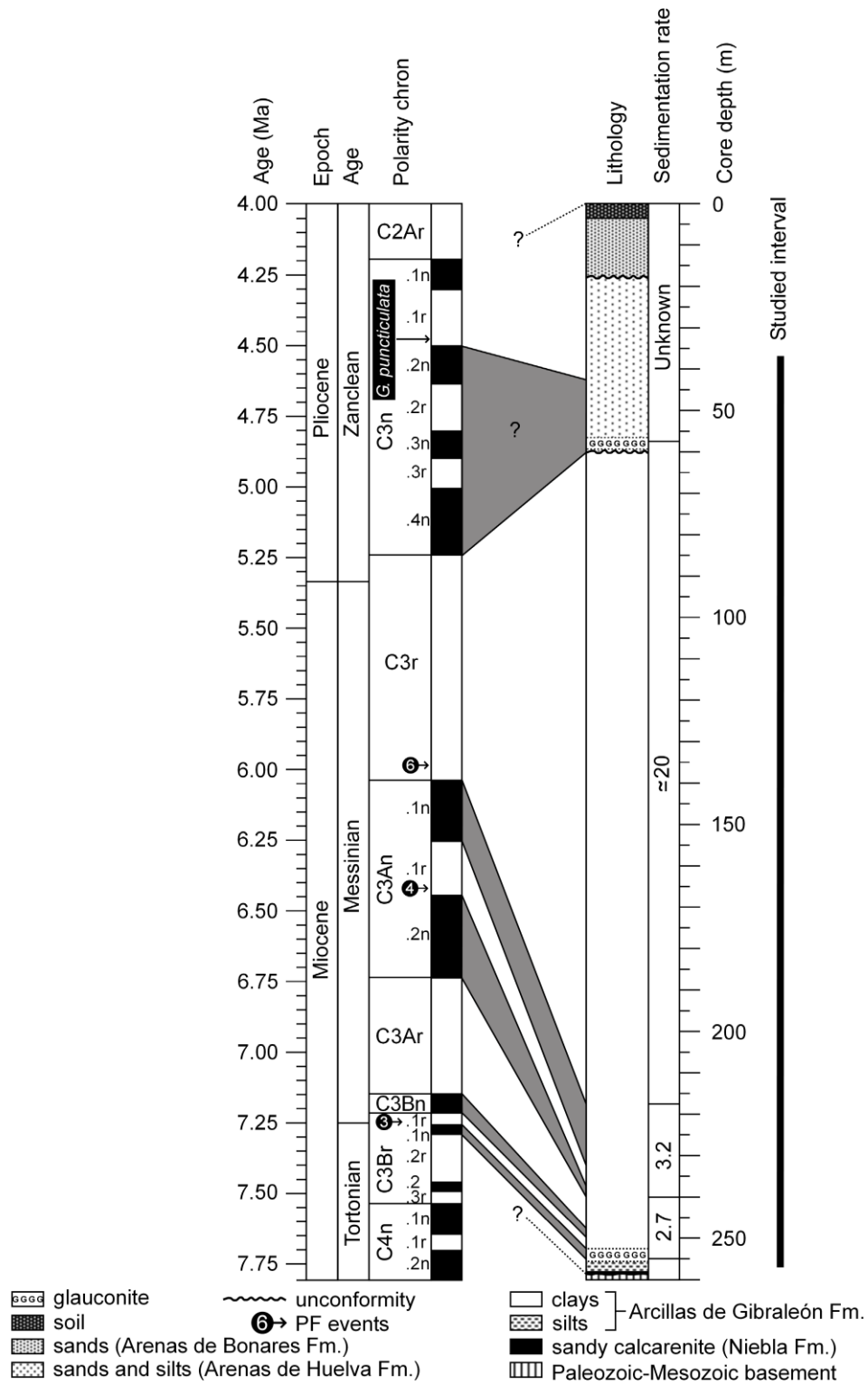


Figure 4

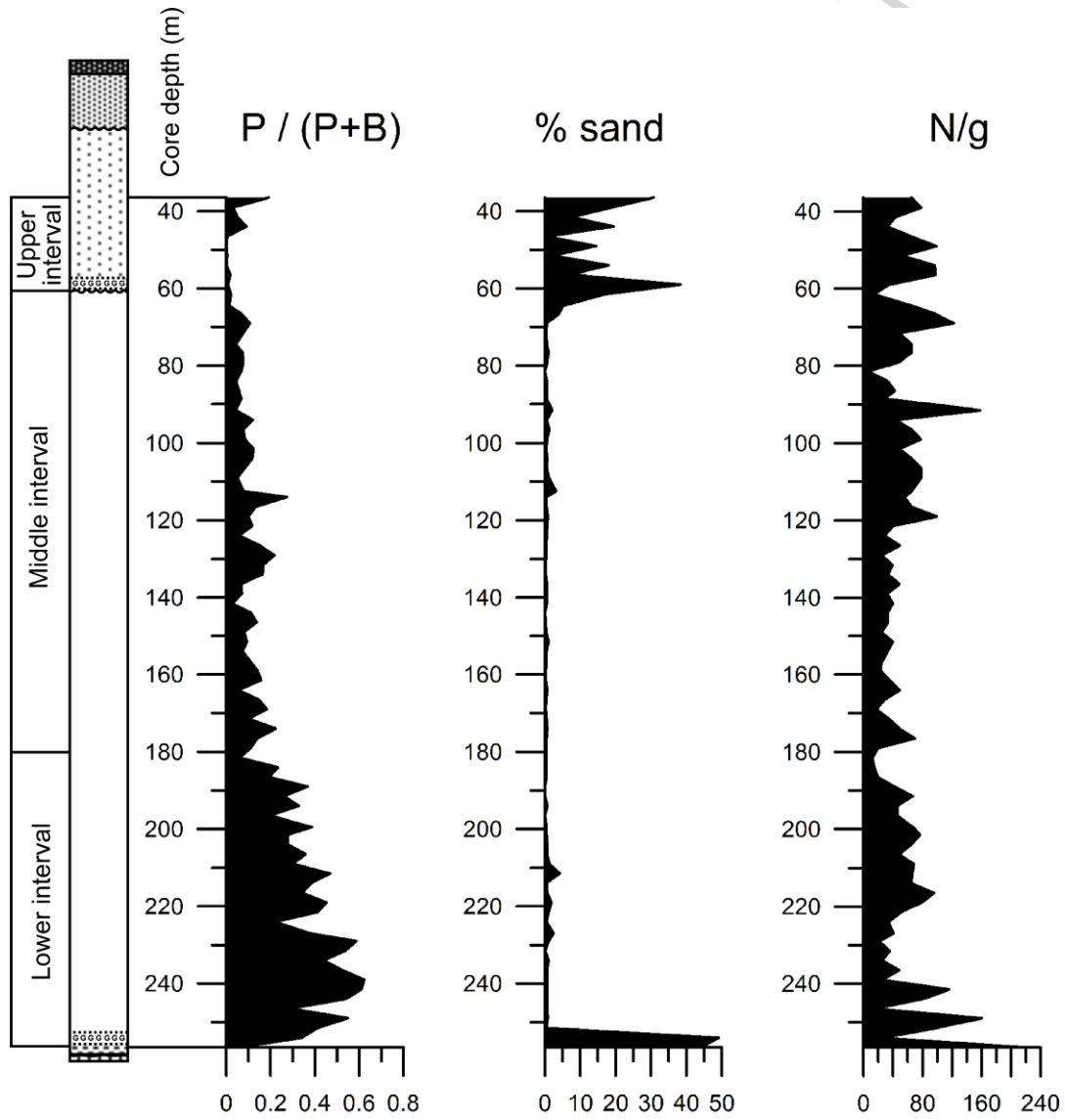


Figure 5

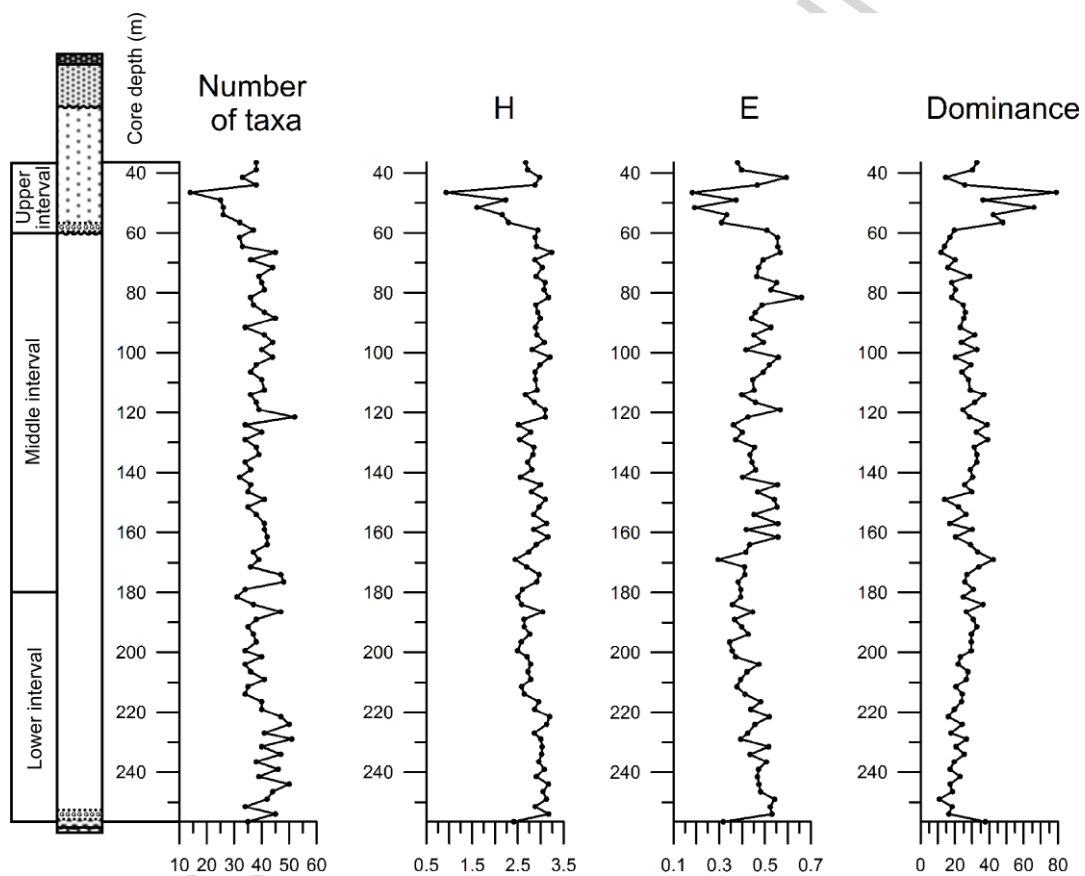


Figure 6

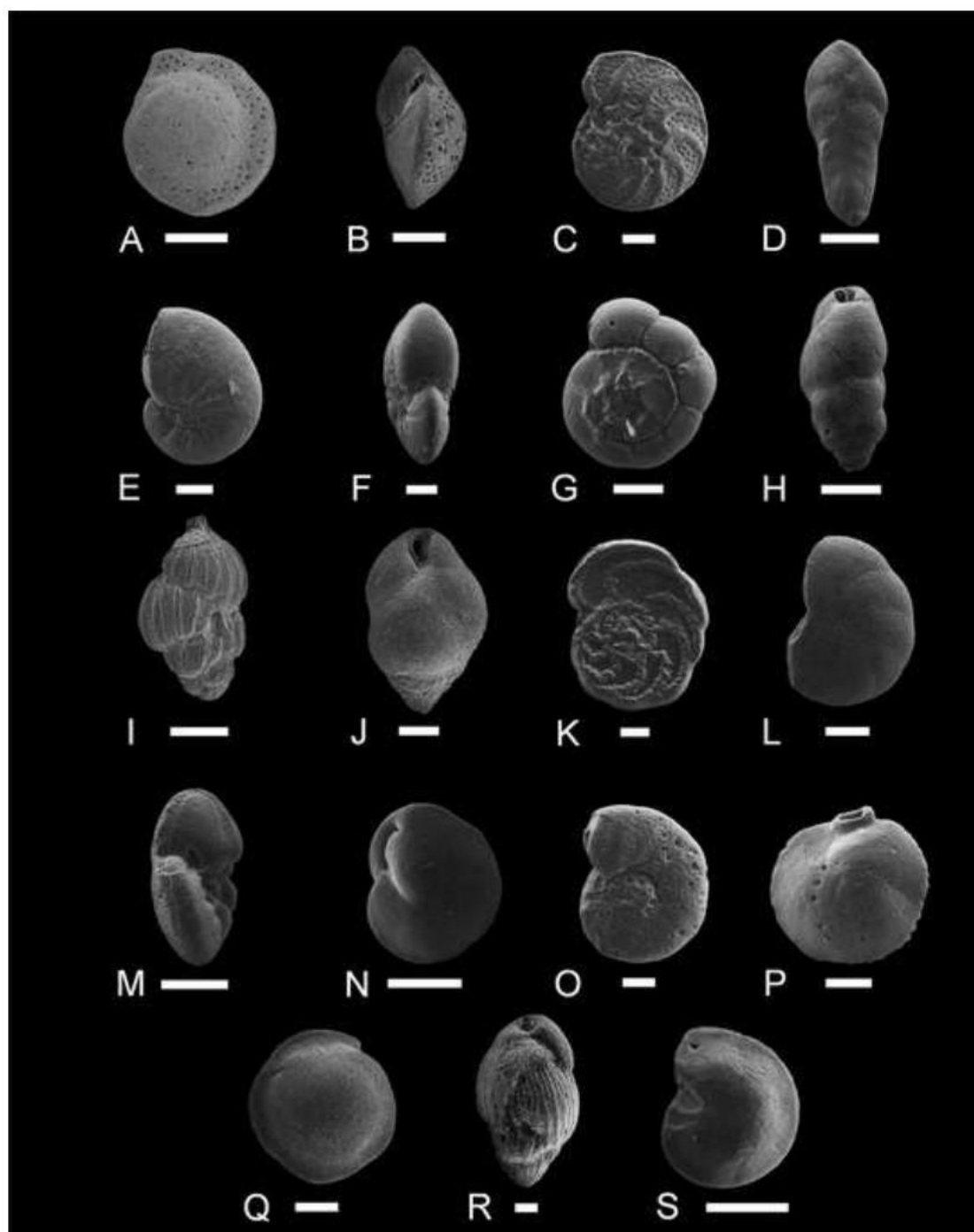


Figure 7

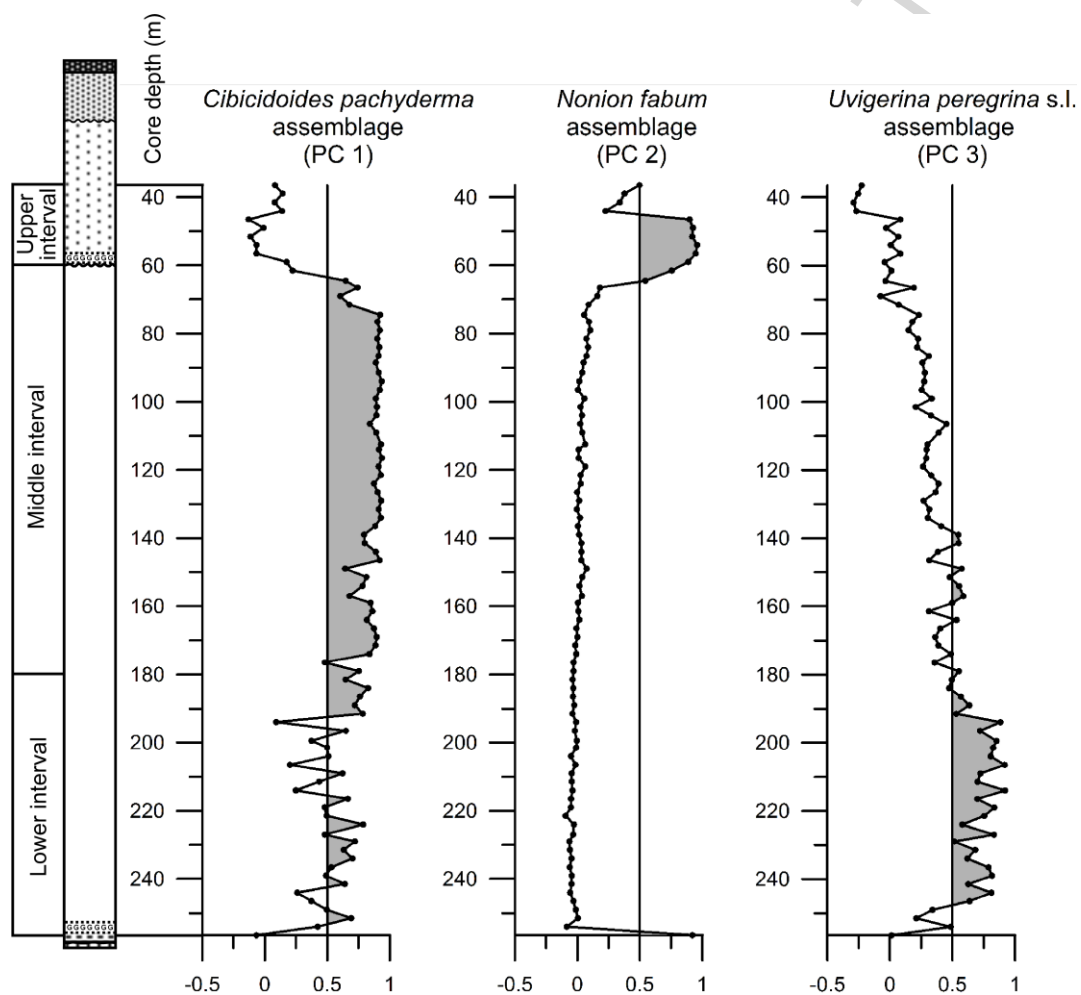


Figure 8

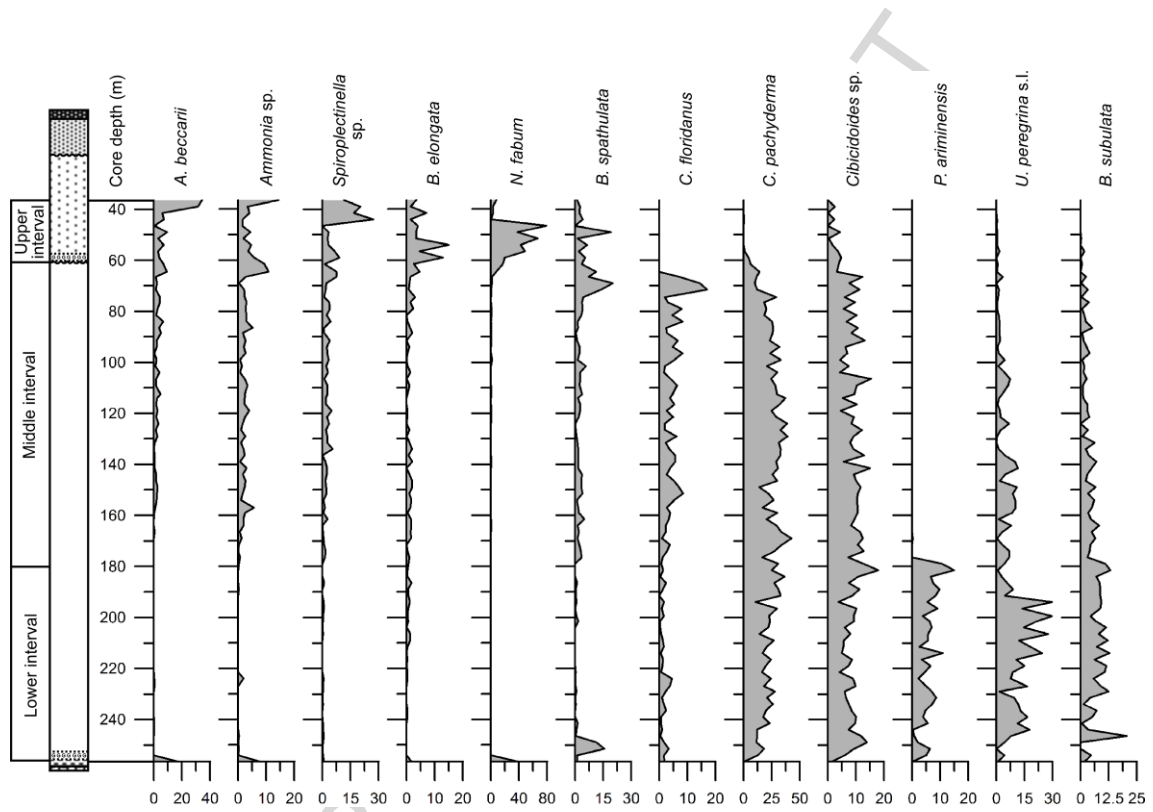


Figure 9

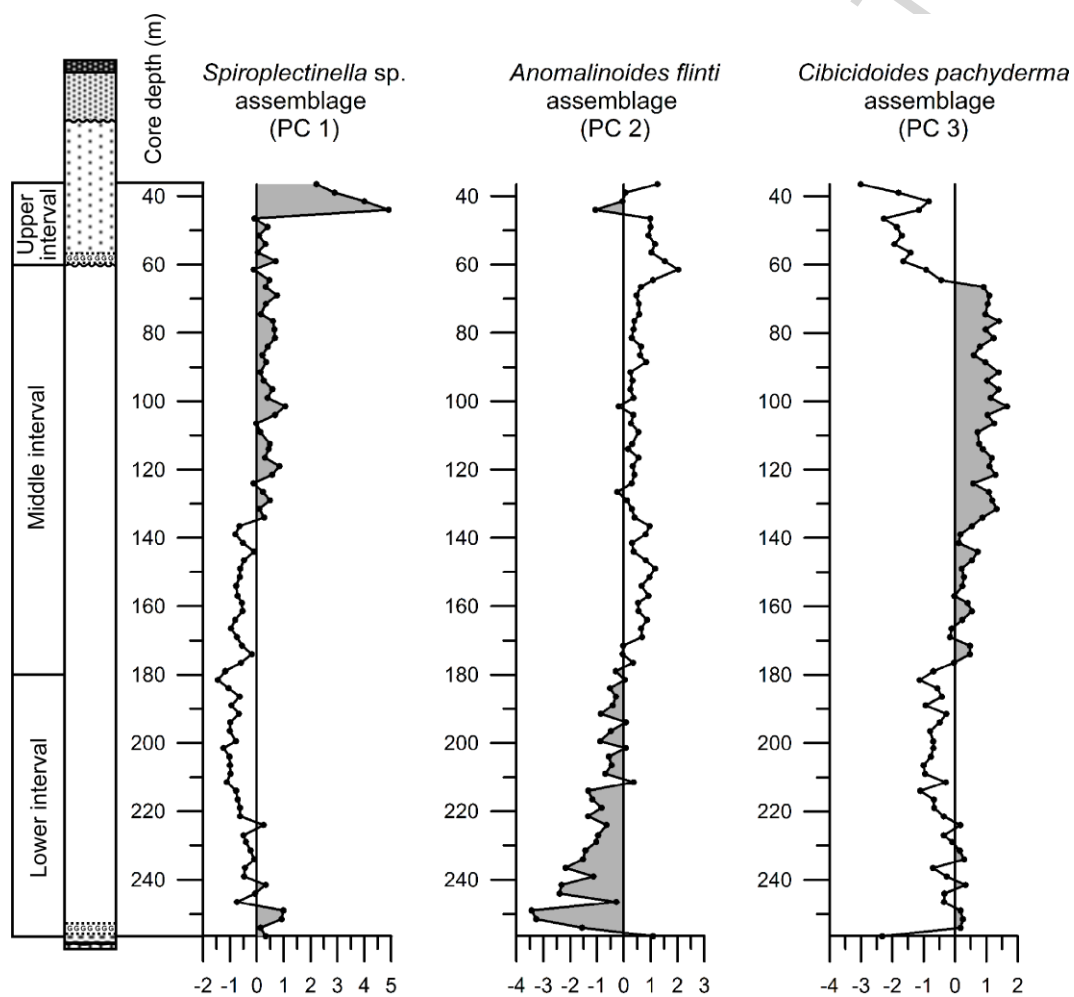


Figure 10

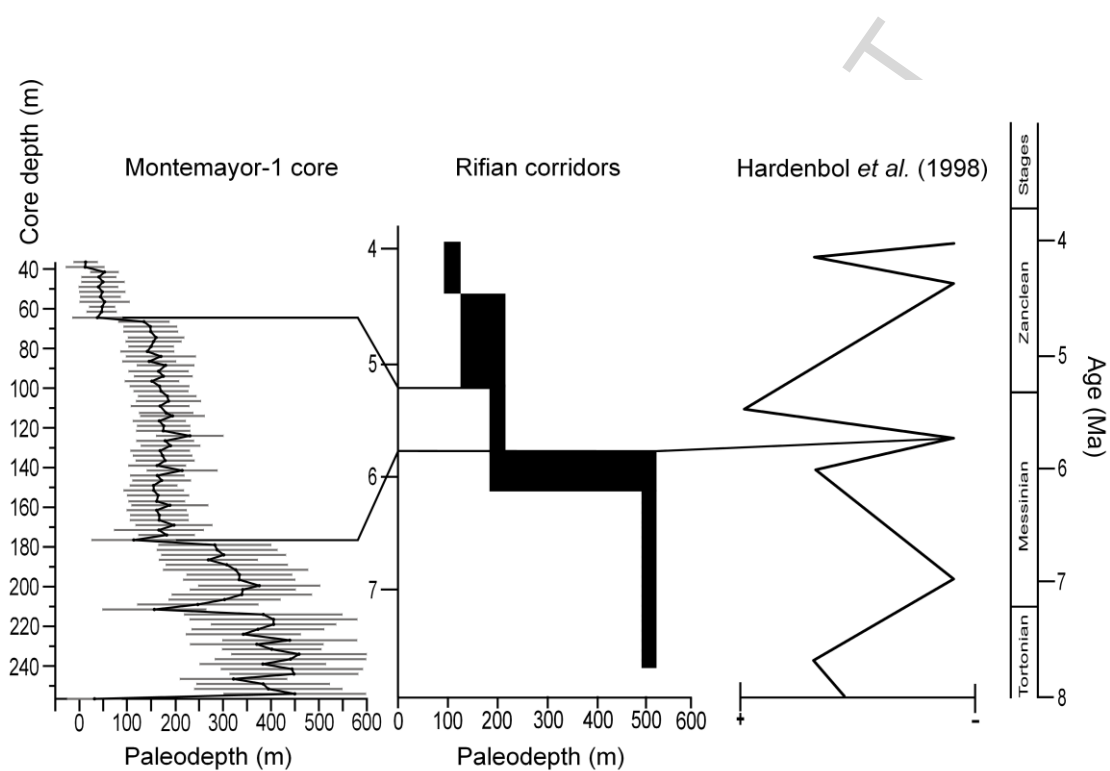


Figure 11

